# A boundary vector cell model of place field repetition

Roddy M. Grieves[1], Éléonore Duvelle[1], Paul A. Dudchenko[2,3]

[1]University College London
Institute of Behavioural
Neuroscience
Department of Experimental
Psychology
London,
United Kingdom

[2]School of Natural Sciences,
University of Stirling,
Stirling,
United Kingdom

[3]Centre for Cognitive and
Neural Systems,
Edinburgh Medical School:
Biomedical Sciences,
University of Edinburgh,
Edinburgh,
United Kingdom

# 1 Abstract

2 Hippocampal place cells are thought to form the neural substrate of a global cognitive map.

3 However, in multicompartment mazes these cells exhibit locally repeating representations,

4 undermining the global cognitive map view of place cells. This phenomenon appears to be

5 related to the repetitive layout of these mazes, but still no hypothesis adequately explains it.

6 Here, we use a boundary vector cell model of place cell firing to model the activity of place cells

7 in numerous multicompartment environments. The activity of modelled place cells bears a

8 striking resemblance to experimental data, replicating virtually every major experimental result.

9 Our results support the boundary vector cell model and indicate that locally repeating place cell

10 firing could result purely from local geometry.

11

# Introduction

**Place cells**

Place cells are neurons in the hippocampus that increase their firing rate when an animal visits specific regions of its environment (O'Keefe, 1979; O'Keefe & Conway, 1978; O'Keefe & Nadel, 1978). Different place cells have 'place fields' in different areas of an environment, so that together the entire surface of an environment is represented (O'Keefe, 1976; Wilson & McNaughton, 1993). The main argument of the current work is that place fields are driven by local geometric features, for example the walls of a maze. To test this, we used a computational model based on inputs to place cells from cells that encode the distance and direction of local boundaries.

Several properties of place cells make them an ideal neural substrate for spatial navigation (O'Keefe & Nadel, 1978) and memory (Eichenbaum et al., 1999). For example, once a place field has formed, it is stable across days (Muller, Kubie, & Ranck, 1987) and even weeks (Thompson & Best, 1990). If an environment is altered or completely novel, place cells may change their firing relationship, forming a representation seemingly unique to this space (O'Keefe & Conway, 1978; Alme et al., 2014), a process known as 'remapping' (Anderson & Jeffery, 2003; Leutgeb et al., 2005; Muller & Kubie, 1987). Remapping can be induced by changing the geometry of an environment (Muller & Kubie, 1987), or by changing the color of a visual cue (Bostock et al, 1991) or an environment's walls (Kentros et al, 2004; Anderson & Jeffery, 2003). Hippocampal activity can be used to decode the current position of an animal in real-time (Pfeiffer & Foster, 2013) and has been implicated in the planning of future trajectories (Bendor & Spiers, 2016; Grieves et al. 2016a; Pfeiffer & Foster, 2013). Similar activity is also apparent during sleep, where it is thought to underlie memory consolidation (Girardeau et al. 2009). As we will consider below, however, there are properties of place fields that are inconsistent with a global spatial representation.

**Place field repetition**

Place cells, when recorded in multicompartment and multialleyway environments, express multiple firing fields in similar locations within each sub-compartment. For instance, Skaggs and McNaughton (2005), Fuhs et al. (2005) and Tanila (1999) all demonstrated that, in two identical compartments connected by a corridor or a doorway, many place cells represent the two compartments more similarly than would be expected by chance (Figure 1). Similarly, Spiers et al. (2015), Grieves et al. (2016b) and Harland et al. (2017) extended this apparatus to four compartments and observed repeating place fields (Figure 1). Carpenter et al. (2015) reported the same phenomenon in grid cells and Derdikman et al. (2009) reported that both grid and place cells simultaneously exhibit repeating fields in up to five parallel alleyways with the same orientation. Frank et al. (2000) and Singer et al. (2010) found similar results in multialleyway mazes. For a review of the literature surrounding this phenomenon, see Grieves et al. (2017).

The spatial map formed from these repeating, local representations is unlikely to be optimal for non-local spatial navigation. Indeed, computational analysis suggests that repeating place fields provide poor information for decoding an animal's position (Spiers et al. 2015) and experimental evidence suggests they are accompanied by spatial learning deficits (Grieves et al., 2016b). Why place cells form these repeating representations is largely unknown. While field repetition is likely linked to the repetitive design of these environments, it does not seem to result from identical visual inputs because both Derdikman et al. (2009) and Grieves et al. (2016b) observed repeating fields despite providing distal cues that should have polarised at least some compartments or alleyways. Repeating fields can also be observed in environments

59    without illumination (Grieves, 2015). Likewise, repeating place fields cannot be due to place

60    cells encoding body movements or response sequences in a stereotyped task because they can

61    be observed in environments where animals are free to explore and behave naturally (Grieves

62    et al., 2016b; Spiers et al., 2015). Moreover, this phenomenon does not seem to be purely due

63    to disorientation in vastly ambiguous environments since place field repetition can be seen in as

64    little as two (Fuhs et al., 2005; Skaggs & McNaughton, 1998; Tanila, 1999) and as many as five

65    (Derdikman et al., 2009) compartments. Yet, a common feature in each of these experiments is

66    repetitive local compartments. Thus we hypothesise that geometry must play a fundamental role
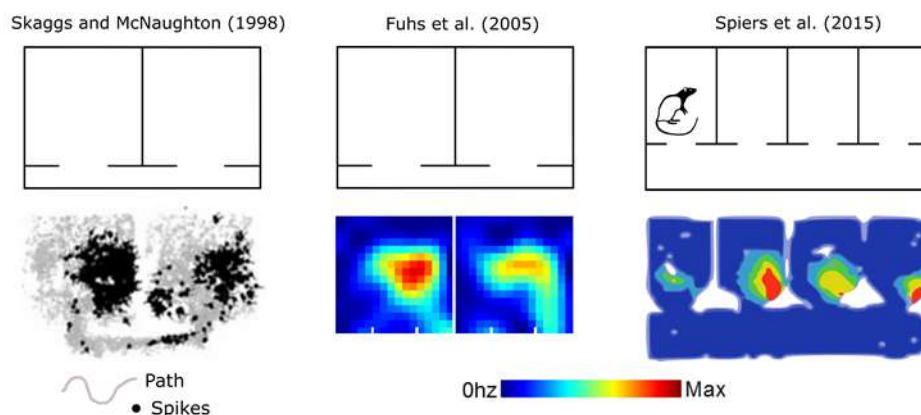
67    in the repetition of place fields.



**Figure 1** Mazes where repeating place field patterns have been observed. ***Top row***; floor plan maze diagrams. ***Bottom row***: the response of a single neuron either showing the path of the animal and the position of the cell's action potentials or a firing rate map of the cell's activity.

68

69    **BVCs and boundary cells**

70    To initialise and maintain a consistent spatial map, place cells appear to rely on distal

71    cues or landmarks surrounding an environment. If these landmarks are rotated, the firing fields

72    of place cells rotate correspondingly (Muller & Kubie, 1987; O'Keefe & Conway, 1978;

73    Yoganarasimha & Knierim, 2005). However, place cell firing also appears to be influenced by

74   the geometry of an environment. For instance, when elongating a square environment into a

75   rectangle, previously small and round place fields can be seen to stretch in proportion to the

76   walls, becoming long and distended (O'Keefe & Burgess, 1996) and place cells recorded in

77   differently shaped, but resembling environments often appear to have place fields in similar

78   locations (Lever, Wills, Cacucci, Burgess, & O'Keefe, 2002). These geometric determinants led

79   researchers to formulate a model of place cell firing which employed hypothetical Boundary

80   Vector Cells (BVCs). BVCs fire in relation to environmental boundaries at a specific distance

81   and direction from an animal (Figure 2). The sensitivity of these cells is controlled by distal cues

82   (i.e., visual cues that are not directly accessible by the animal) and place cell firing has been

83   proposed to arise from the thresholded sum activity of a subpopulation of BVCs (Barry et al.,

84   2006; Burgess, Donnett, Jeffery, & O'Keefe, 1997; Burgess, Jackson, Hartley, & O'Keefe, 2000;

85   Hartley, Burgess, Lever, Cacucci, & O'Keefe, 2000; Lever, Burgess, Cacucci, Hartley, &

86   O'Keefe, 2002)(Figure 3). This model explains very well the geometric features of place cell

87   firing.

88
89        Following the introduction of the BVC model, neurons similar to BVCs have been

90   observed in a number of brain regions including the subiculum (Barry et al., 2006; Lever,

91   Burton, Jeewajee, O'Keefe, & Burgess, 2009; Sharp, 1999; Stewart, Jeewajee, Wills, Burgess,

92   & Lever, 2014), parasubiculum (Boccara et al., 2010; Solstad, Boccara, Kropff, Moser, & Moser,

93   2008), medial entorhinal cortex (mEC)(Bjerknes, Moser, & Moser, 2014; Savelli,

94   Yoganarasimha, & Knierim, 2008; Solstad et al. 2008) and recently the rostral thalamus

95   (Jankowski et al., 2015) and anterior claustrum (Jankowski & O'Mara, 2015) (Figure 2). These

96   'boundary' cells have a preferred firing direction, much like head direction cells, but instead of

97   firing maximally when the animal's head is facing this direction, a given boundary cell will fire

98   when an environmental boundary lies in that direction from the animal. This firing is driven by

99   the boundary's position relative to the animal, presumably based on self-motion information.

100 Consistent firing is observed in every environment where the cell is recorded, provided that the

101 external reference frame is maintained.  For instance, consistent boundary fields are anticipated

102 if each environment is placed in the same curtain enclosure with the same distal cue card

103 (Lever et al., 2009; Sharp, 1997). Environmental boundaries which can drive cell firing in this

104 way may be walls, low ridges or vertical drops and the colour, texture or odour of these does not

105 seem to influence the cell's firing (Lever et al., 2009).

106     The proposition that place cell firing may be the result of boundary cell input as opposed

107 to other cell types such as grid cells has gained recent support (Barry & Burgess, 2007; Bush,

108 Barry, & Burgess, 2014; Hartley, Burgess, Lever, Cacucci, & O'Keefe, 2000). At 2.5 weeks of

109 age, rat pups already have an internal representation of their environment in the form of

110 relatively stable place fields capable of remapping (Muessig et al. 2016) and a fully functional

111 head direction signal. However, their grid cells have still not fully developed a hexagonal grid

112 firing pattern (Bjerknes, Moser, & Moser, 2014; Langston et al., 2010) and do not exhibit them

113 until 3 weeks of age (Wills, Barry, & Cacucci, 2012). In contrast, before 2.5 weeks of age

114 boundary cells in the mEC are already fully developed (Bjerknes et al., 2014) and place cell

115 activity is significantly more stable near to environmental boundaries (Muessig et al. 2015).

116 These findings, in conjunction with the accuracy with which BVC models can account for and

117 even predict place cell firing in multiple environments suggests that boundary cells play a role in

118 the development, formation and maintenance of hippocampal spatial representations.

119     If geometry plays a role in the repetition of place fields, utilising a purely geometric

120 model of place cell activity based on BVCs should explain why we observe repetition in

121 multicompartment and multialleyway environments. By their very definition, boundary cells are

122 sensitive to environmental geometry and a model in which place cell firing is at least partially

123 dictated by their inputs should also predict the pattern of results observed in the

124 multicompartment environments described above. Thus, we predict that if place field repetition

125 is purely the result of local geometry then we should be able to accurately model the activity of

126    place cells in each of the environments described above using only geometric inputs. If this is

127    the case it would indicate that place cells preferentially utilise local, geometric information which

128    is then stitched together to form a larger 'map' of an environment. This would undermine the

129    view that the hippocampus forms a unified global cognitive map of complex environments – at

130    least initially - because it suggests large scale spatial representations in the brain are actually

131    composed of small scale geometric ones. If the model is inaccurate, however, this would

132    suggest that repetitive local geometries are not sufficient to drive place field repetition.
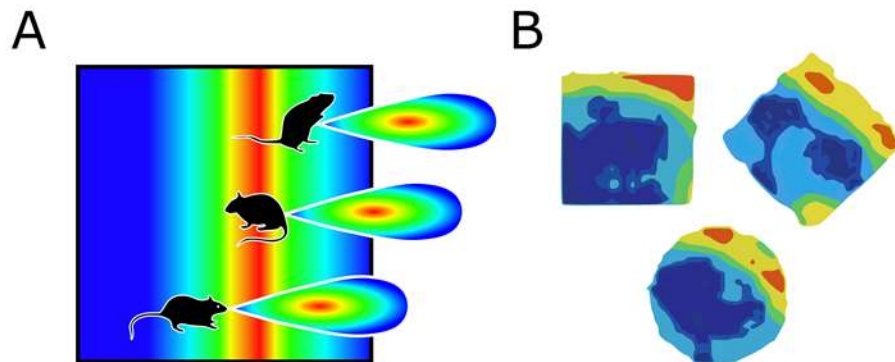
133

134

135



**Figure 2** Implementation of the boundary vector cell model. *A,* figure adapted from Barry et al. (2006) describing the overlapping Gaussians contributing to the firing of a BVC sensitive to boundaries found an angle of 0° to the rat and at a distance of 30cm. The right boundary of this environment satisfies the directional component of the BVC. As the rat moves towards and away from it, firing increases and decreases depending on its preferred firing distance. *B,* firing rate maps for a single boundary cell recorded in the subiculum in a square, diamond and circular environment (adapted from Lever et al. (2009), figure 3, cell 2d).

136

137

# Overall Methods

**The BVC model**

As in Hartley et al. (2000) and Barry et al. (2006), the spatially receptive bounds of our BVCs were modelled as the product of two Gaussians. One varies as a function of the rat's distance from a boundary, the other varies as a function of the angle this boundary presents at the rat. To implement this, we created scale models of the environments reported in the literature and partitioned these into pixels such that each pixel was equivalent to 1 cm square. Then, for every pixel in the environment, for every direction in the range (0, 2π], we calculated the distance ($r$) from the pixel to the nearest boundary segment at that direction ($\theta$) and the angle ($\Delta$) that segment subtended to the pixel. Thus, for a given BVC$_i$ that is optimally responsive to boundaries at a distance $d_i$ and at an angle $\alpha_i$ relative to the rat, the receptive field would be described by:

$$f_i(r, \theta, \Delta) \propto \frac{\exp\left(-\frac{(r - d_i)^2}{2\sigma_{rad}^2(d_i)}\right)}{\sqrt{2\pi\sigma_{rad}^2(d_i)}} \times \frac{\exp\left(-\frac{(\theta - \alpha_i)^2}{2\sigma_{ang}^2}\right)}{\sqrt{2\pi\sigma_{ang}^2}} \times \Delta$$

To generate an overall map of the cell's activity for an environment the above equation is applied to every pixel, for all directions in the range (0, 2π] and each pixel's overall value is the linear sum of these results. In this way, all boundaries visible by direct line of sight contribute to the firing of the cell at any given position.

Parameter $\sigma_{ang}$ is a constant which describes the extent of the cell's angular tuning width and $\sigma_{rad}$ is a variable parameter which describes the cell's sensitivity to boundaries in terms of distance. This varies in a linear way with distance such that cells with a larger preferred firing distance have wider firing fields. This linear increase is described by:

$$\sigma_{rad}(d_i) = (d_i / \beta + 1)\sigma_0$$

160    where β and $\sigma_0$ represent constants which determine the rate at which the field increases in size

161    with distance and the radial width of the field at a distance of 0 cm, respectively.

162    **Generating place cells**

163    As in Hartley et al. (2000), we modelled the activity of place cells as the combined input

164    of 2 or more BVCs. However, rather than generating place cells as the linear sum of *n* BVCs, as

165    is the case in previous BVC models, we chose to calculate the geometric mean (Figure 3). This

166    consists of taking the *n*th root of the product of *n* BVCs and is given by:

167
$$F(x) \;=\; u\left(\left(\prod_{i=1}^{n} f_i(x)\,/\,max_x\right)^{\frac{1}{n}}\right) - T$$

168    where *F* is a place cell, $f_i$ is a BVC, *x* is a location in the rate map of the cell, *T* is the cell's

169    threshold and *u* represents a Heaviside step function ($u(x)$ = x, if x > 0, otherwise $u(x)$ = 0)

170    (Barry et al., 2006). In this way, *T* and *u* act together as a linear threshold on the cell's output.

171    Calculating the product of BVCs results in much better spatial tuning of the resulting place cell

172    and accurately captures much of the features seen in vivo, especially in tight alleyway mazes

173    which compose half of the environments modelled here. Multiplicative neural processes have

174    been reported previously (Peña & Konishi, 2001; 2004), thus it is possible that boundary cell

175    inputs act multiplicatively on postsynaptic place cells (Schnupp & King, 2001), although

176    evidence for this has not yet been shown. One problem is that, as the number of BVCs

177    increases, the resulting place cell activity decreases as a power function of the inputs. The

178    geometric mean therefore acts to normalise the result of this product and was used primarily for

179    this purpose - we note that linear summation and multiplication alone produce similar results to

180    those reported here (data not shown). As a further step we also multiplied *F(x)* by 500 in order

181    to scale the majority of PC spatial maps so that their maximum fell between 1 and 20Hz which

182    are generally accepted cutoffs for place cells (Grieves et al., 2016b). However, a different

183    coefficient could be used to better model the proportion of active and silent cells in a given

184    environment (Thompson & Best, 1989). Note also that BVCs are normalised between 0 and 1

185    (by division of their maximum, $max_x$), meaning that each BVC contributes equally to the firing of
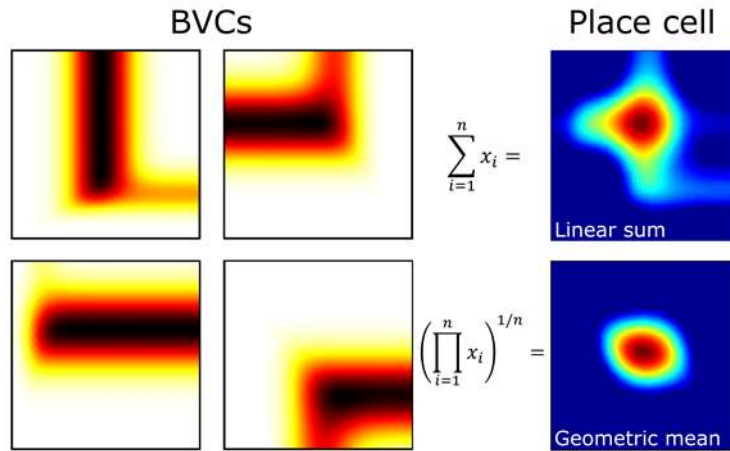


**Figure 3** A geometric mean approach to combining BVC inputs. ***Left,*** activity of four modelled BVCs in a 128cm square. ***Top right***, result combining BVC information by linearly summing across all four BVC ratemaps. ***Bottom right***, geometric mean result. Both place cell maps have been produced using the same final threshold (30% of the maximum), however, the geometric mean approach yields a more spatially tuned response.

186    a place cell.

187

188        In another departure from earlier implementations of the BVC model, instead of drawing

189    BVC preferred distances from a discrete distribution (Hartley et al., 2000) we selected distances

190    from a continuous Gaussian constrained between 6 and 256 cm (μ = 0 cm, σ = 100 cm). This

191    largely biases the population of BVCs towards shorter preferred firing distances which better

192    represent the population of BVCs found in the subiculum (Lever et al., 2009) and border cells in

193    the mEC (Savelli, Yoganarasimha, & Knierim, 2008; Solstad et al., 2008). Preferred firing angles

194    were selected randomly from the uniform distribution (0, 2π]. Each place cell was modelled as

195    the geometric mean of $n$ BVCs where $n$ was drawn from a Poisson distribution constrained

196    between 2 and 16 (λ = 4 cells). We reasoned that the brain generates place cells using as few

197    connections and computations as possible and, in reality, this distribution does not often exceed

198    10 inputs. However, we note that varying the number of inputs of our geometric mean model

199    does not change the overall results and place cells can be generated reliably using 2 to 24

200    BVCs. It may be desirable to select BVCs non-randomly based on their preferred firing direction,

201    to prevent generating place cells using 2 BVCs with very similar firing patterns. We did not

202    implement this constraint for computational simplicity and because this is not an obvious

203    biological trait of the subicular inputs to the hippocampus.

204          We modelled the activity of place cells and BVCs in several environments, some of

205    which were open-field control environments where we sought to demonstrate the functionality of

206    the model, such as square (64 x 64cm and 128 x 128cm) and rectangular (64 x 128cm and 128

207    x 64cm) environments similar in size to those used by Lever et al. (2009) and O'Keefe and

208    Burgess (1996). We also used circular environments (64cm and 128cm in diameter) similar in

209    size to those used by Muller and Kubie (1987) or to a watermaze (Morris, 1981) respectively.

210    We also modelled a 64cm square environment with a wall extending halfway across its central

211    diameter which has been used previously to demonstrate place field repetition (Barry et al.,

212    2006; Lever, Cacucci, Burgess & O'Keefe, 1999).

213          Additionally, we modelled mazes in which researchers have previously shown place field

214    repetition. These mazes were the two compartment mazes used by Skaggs and McNaughton

215    (1998), Fuhs et al. (2005) and Tanila (1999), the 'hairpin' maze used by Derdikman et al.

216    (2009), the square and circular spiral tracks used by Nitz et al. (2011) and Cowen and Nitz

217    (2014), the four compartment mazes used by Spiers et al. (2015), the two configurations used

218    by Grieves et al. (2016b) and a multi-alleyway maze similar to that used by Frank et al. (2000),

219    Singer et al. (2010) and Grieves (2015).

220          For the purposes of this study we generated 10,000 BVCs in each of these

221    environments such that a spatial map was produced for each BVC in every environment. The

222    preferred firing distances and directions were maintained for these BVCs across environments,

223    thus, a change in a given BVC's spatial activity between environments is due to changes in the

224    structure of the environment rather than a change in the cell's characteristics. We then

225    generated 1,500 place cells in all environments. Each place cell received consistent BVC inputs

226    across all environments, and thus differences in place cell firing were due to changes in

227    underlying BVC activity rather than changes in BVC connectivity.

228    **Place field analyses**

229    Unless otherwise stated, all analyses were performed on the unsmoothed firing rate

230    maps produced using the above method, generated at a pixel resolution where 1 pixel = 1 cm$^2$.

231    When detecting place fields, we looked for areas of more than 9 contiguous pixels with a firing

232    rate greater than 20% of the maximum value in the ratemap. The area, position (taken as the

233    weighted centroid), dimensions and firing rate properties of these fields were then extracted and

234    their ellipticity calculated. Ellipticity was defined as the ratio between the major and minor axis

235    lengths:

236    $$\varepsilon = \frac{\alpha - \beta}{\alpha} = 1 - \frac{\beta}{\alpha}$$

237    where α represents the length of the semi-major axis and β represents the length of the semi-

238    minor axis' length. This gives a measure of the curvature of the place field, such that an

239    ellipticity of 0 would represent a circle and an ellipticity of 1 would represent a straight line

240    (although these are degenerate cases).

241    **Morphing**

242    For morphing analyses we used an algorithm described previously (Lever et al., 2002).

243    Briefly, we found the correspondence such that each point maintains its radial position as a

244    proportion of the distance to the perimeter along that radius. For instance, if we wish to morph

245    map 1 ($m_1$) into the shape of map 2 ($m_2$) we can achieve this using an inverse lookup

246    transformation whereby we fill each pixel of map 2 using the closest pixel in map 1. For our

11

247 method we defined the closest pixel as the one with the same angle from the centre of the map

248 ($\theta$) and the same ratio of distance from the centre to the edge ($r$). From this it follows that for all

249 points in $m_2$:

250 $$m_2(r, \theta) = m_1(r, \theta)$$

251 See figure 4A for a schematic of this procedure.

252

# 253 Open field environments

254       A geometric model of place cell firing carries a number of basic predictions that we

255 sought to verify in our own modelled place cell data. For instance, one prediction of the BVC

256 model is that place cells should exhibit similar representations for environments of different

257 shapes (Hartley et al., 2000; O'Keefe & Burgess, 1996). Lever et al. (2002) demonstrated this

258 effect by showing that place cells in square and circular environments containing the same

259 visual cue had very similar firing rate maps (at least initially), when the rate map of one

260 environment was 'morphed' into the shape of the other. O'Keefe and Burgess (1996) similarly

261 demonstrated that place cells recorded in a square environment often exhibit distended or

262 elongated firing fields when the environment was stretched along one dimension and suggested

263 that this response could be explained in terms of a boundary interaction on place cell firing.

264 Conversely, if instead of being stretched an environment is bisected in half by a barrier, place

265 cells will often fire similarly in the spaces on either side of it (Barry et al., 2006), provided that

266 those spaces share a similar local geometry (Paz-Villagrán, Save, & Poucet, 2004).

267       **Methods for open fields**

268       We modelled the activity of place cells in a small square, diamond and circular

269 environment (all 64cm in length or diameter) and in a large square and circular environment

270 (both 128cm in length or diameter). For each place cell we then morphed the activity in each

271 environment into the shape of every other environment using the method described above. We

272    then correlated these maps to determine how similarly cells represent environments of different

273    shapes and sizes. We also compared the median place field area and ellipticity of these cells in

274    a small square, large square and two rectangles elongated along each dimension as reported

275    by O'Keefe & Burgess (1996). Finally, we modelled the activity of cells in a 64cm square

276    bisected by a 32cm barrier and calculated the level of correlation between the two halves of the

277    environment divided along this barrier. We compared this distribution to one calculated using

278    the same method on a square environment with no barrier.

279    **Results for open fields**

280    *Place fields do not expand in proportion to the environment, and similarly sized*
281    *environments are represented similarly*

282    In the diamond, small square, large square, small circle and large circle environments

283    we observe a similar proportion of active (firing > 1Hz) cells (1209 or 19.4%, 1212 or 19.2%,

284    1207 or 19.5%, 1178 or 21.5%, 1106 or 26.3% respectively; $z = 15$, $p > .05$, Wilcoxon signed

285    rank test) and cells exhibit a similar number of place fields in each environment (Md = 1 in all

286    cases). However, we find that place fields do not expand in direct relation to the size of the

287    environment. For instance, the mean ratio between field area in the small and large square

288    environment is 1.8, not 4 as would be expected based on the surface area of the environments

289    and between the circular mazes it is 1.9 (expected would be 4). When comparing the morphed

290    spatial firing maps for these environments, they are all more similar than would be expected by

291    chance ($p < .0001$ and $r > 0.3$ in all cases, Wilcoxon rank sum tests (WRSt)). However,

292    morphed versions of similarly sized environments are consistently more similar than those of

293    different sized environments ($z = 54.9$, $p < .0001$, $r = 0.45$, WRSt, Md = 0.69 and 0.30

294    respectively) (Figure 4A).
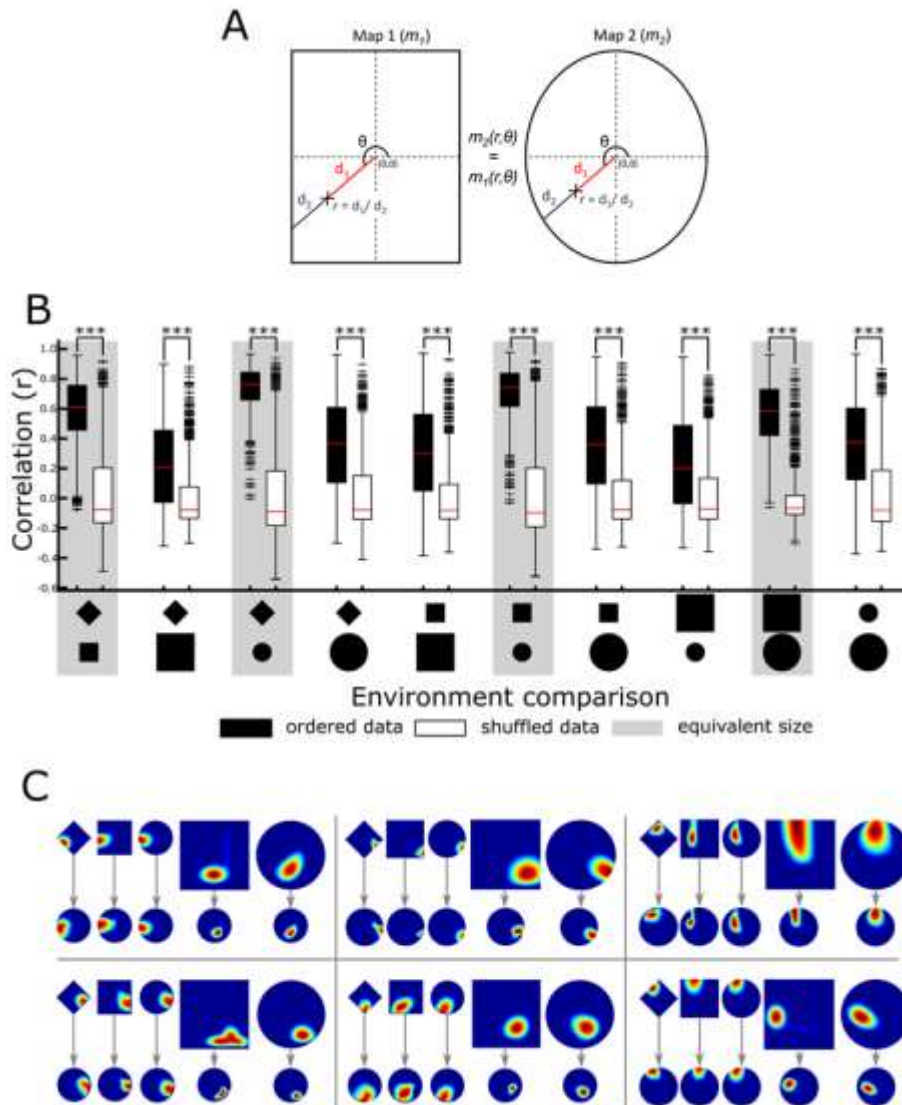
295

**Figure 4** Place cell activity in the open field environments. *A,* schematic of the morphing procedure used. An inverse transformation is used to find pixels in map 1 which can best fill values in map 2, this is more efficient than the reverse process. *B,* distribution of values obtained by correlating the activity of a place cell in each open field environment to the same cell's activity in each other environment, after morphing the first to the same shape as the second. Open boxes indicate shuffled distributions where place cells were morphed and then compared to a random cell's activity in the second environment. Comparisons between environments which were initially the same size, not necessarily the same shape, are the highest (grey shaded comparisons), suggesting that place cells represent environments of corresponding size more similarly, regardless of their geometry. *C,* activity of six example cells, in each of the open field environments (top row) and result of morphing this activity to match the shape of the small circular environment (bottom row). Morphed versions of environments that are the initially the same size appear more similar than morphed versions of differently sized environments.
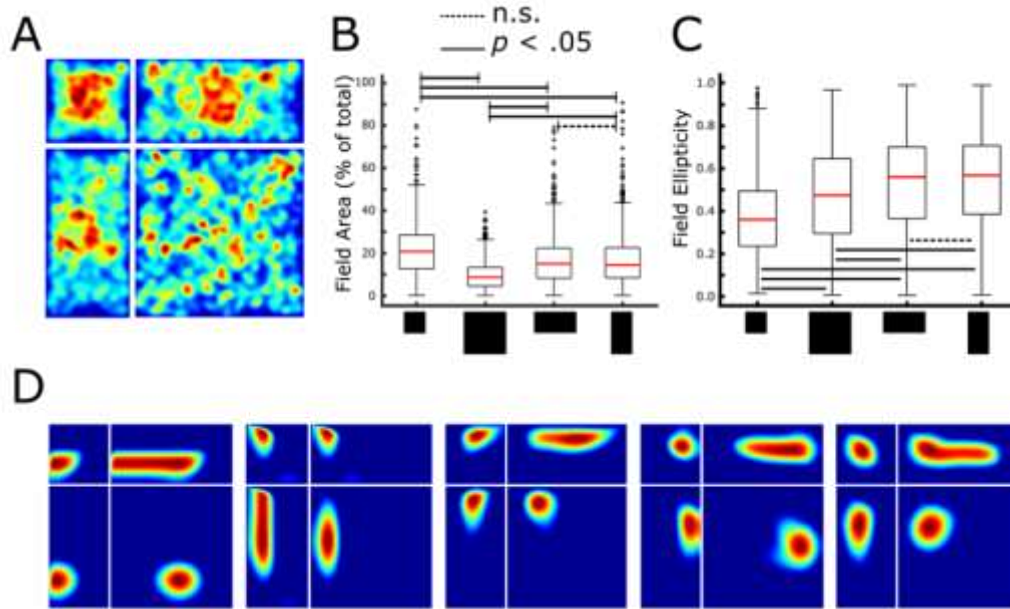
**Figure 5 *A,*** spatial maps of all place fields detected in the four square or rectangular environments. ***B,*** median size of place fields in each environment, expressed as a percentage of the environment's surface area. Fields do not expand to cover a similar proportion of the environment. ***C,*** median ellipticity of place fields in each environment. Place fields have a generally larger ellipticity in the rectangular environments, suggesting that they consistently expand with the environment. ***D,*** activity of four example place cells in all four square or rectangular environments. Each is seemingly sensitive to expansions of the environment in only one dimension.

296            *Elongating an environment results in elongated place fields*

297            The size of place fields differ significantly between the four rectangular and square

298   mazes ($H(3,6469) = 964.5$, $p < 1 \times 10^{-200}$, Kruskal-Wallis test), post-hoc tests confirm that each

299   environment differs from every other ($p < .0001$ in all cases) with the exception of the two

300   rectangular environments ($p > .05$, Md = 15.0 and 14.5, all tests are Mann-Whitney U tests

301   (MWUt) with a Bonferroni correction). The same relationship can be found when comparing

302   place field ellipticity ($H(3,6469) = 574.6$, $p < 1 \times 10^{-120}$, Kruskal-Wallis test) and post-hoc tests

303   again confirm that each environment differs from every other ($p < .0001$ in all cases) with the

304   exception of the two rectangular environments ($p > .05$, Md = 0.56 and 0.57, all tests are MWUt

305   with a Bonferroni correction). As with the previous open field analyses, we also find that place

306     fields do not expand in direct relation to the size of the environment; the observed ratio between

307     the small square and rectangles is 1.6 (lower than the expected ratio of 2)(Figure 5).

308

309         *A bisecting barrier increases place field repetition*

310         In the square environment bisected by a barrier, we found that cells exhibited a

311     significantly higher number of place fields than the same cells in a square open field

312     environment of the same size ($z$ = -24.6, $p$ < .0001, $r$ = -0.43, WRSt, Md = 1 in both cases).

313     Specifically, in the square, cells are more likely to have a single place field, whereas in the insert

314     maze cells were more likely to exhibit two fields. When comparing the half-map spatial

315     correlations we also found that correlations from the barrier maze were significantly higher

316     ($D$(3000) = 0.33, $p$ < .0001, two-sample Kolmogorov-Smirnov test, Md = 0.24 and -0.07

317     respectively), suggesting that the doubling of place fields is a result of the bisecting barrier.

318         **Discussion**

319         As reported by Lever et al. (2002), our modelled place cells represent circle and square

320     environments more similarly than would be expected by chance, but this effect is significantly

321     decreased when the environments are of different sizes. The relationship between environment

322     shape and size has not been expressly tested before, although Muller and Kubie (1987) report

323     that when the diameter of a recording cylinder is enlarged, around 69% of cells are

324     'homotrophic' (i.e. their place field is of a similar size, shape and location relative to the walls).

325     Lever et al. (2002) reported that in two similar sized but differently shaped environments 73% of

326     place cells are homotrophic. Furthermore, when they removed the walls of their circular

327     environment and allowed the animals to explore a larger circular platform, place cells fired much

328     less similarly. This pattern of results clearly seems to follow the results of the current model;

329     place cells represent environments of different shapes similarly, but this effect is stronger when

330     they are also the same size.

16

331    As reported by O'Keefe and Burgess (1996), in a square environment that is enlarged

332    along each dimension independently or both dimensions equally, place fields are significantly

333    more elongated in the rectangular environments than in the squares. As above, we note that

334    place fields in our larger environments are not merely scaled-up versions of the fields in the

335    smaller ones. Muller and Kubie (1987) also reported the same effect in their data; depending on

336    the methods used to generate their firing rate maps they found that, in a large cylinder that was

337    twice the diameter of a small one (and 4 times the surface area), place fields only expanded

338    their area by a factor of about two (values ranged from 0.87 to 2.49) which is very similar to our

339    findings. Thus, place field area is not proportional to the area of the environment.

340    As reported previously by Barry and Burgess (2007), in a square environment bisected

341    by a barrier, our modelled place cells exhibited more place fields than in a similarly sized open

342    square. Furthermore, these cells were found to represent each half of the environment, as

343    bisected by the barrier, more similarly than would be expected by chance. Together, these

344    results confirm that our BVC model correctly predicts many of the geometric features of place

345    cell firing observed in previous experiments.

346
347
348    ## Alleyway mazes

349    A number of experiments have demonstrated that in mazes composed of multiple

350    alleyways, place cells exhibit place fields in similar locations along each alleyway. We propose

351    that, in each case, the firing of place cells is repetitive due to the same process underlying firing

352    in the square environment with a barrier insert. For instance, Frank et al. (2000) and Singer et

353    al. (2010) recorded place cells in a maze composed of 2 to 6 repeating parallel alleyways. In

354    these mazes, place cells expressed multiple place fields in a repeating fashion which was

355    attributed to learning similar responses in different locations (Frank et al., 2000). However, the

356    same phenomenon was observed when rats explored a maze composed of four parallel

357   alleyways for the first time, both in the light and in complete darkness (Grieves, 2015). As

358   boundary cells respond similarly to vertical drops as they do to physical walls, it may be that

359   their inputs can account for place field repetition in these types of mazes.

360        In another multialleyway experiment, Derdikman et al. (2009) showed that in a linear

361   track composed of multiple alleyways that zig-zag back and forth through space, called a

362   'hairpin' maze, place cells exhibited place fields in similar locations along multiple alleys.

363   However, they also found that these fields tended to occur at roughly the same distance along

364   each alleyway and only in those alleyways which faced the same direction (i.e. in every second

365   alleyway or in every alley where the rat faced south). This result is seemingly in contradiction to

366   the BVC model as local geometry does not seem to change significantly between alleyways.

367   Still, Derdikman et al. (2009) showed that field repetition persisted in rats trained in the same

368   maze with transparent walls, but not in rats trained to run in a stereotypical manner in an open

369   field, implicating the physical walls of the maze and thus local geometry.

370        In a similar demonstration of the importance of angular head direction, Nitz et al. (2011)

371   found that, when rats run along a track which spirals inwards on itself, place cells often had

372   multiple place fields positioned in different 'coils' of the spiral and arranged at a consistent angle

373   with relation to the centre of the maze. As with the open field environments, we sought to

374   replicate these findings in our modelled place cell population.

375        **Methods**

376        We modelled the activity of cells in a maze composed of four parallel alleyways as this

377   best represented the mazes of Frank et al. (2000), Singer et al. (2010) and Grieves (2015). To

378   quantify place field repetition, for each cell we calculated the spatial correlation between each

379   pair of alleyways in the maze and compared this to a distribution of spatial correlation values

380   calculated by comparing alleyway maps from different cells. This shuffle was performed without

381   replacement. In all cases, a correlation was computed only if the firing rate in each alleyway

382  map was greater than 1 Hz. We also modelled the activity of place cells in a scale reproduction

383  of the hairpin maze used by Derdikman et al. (2009) and in an open field environment of the

384  same outer dimensions. We then performed a 1-dimensional autocorrelation whereby ratemaps

385  were shifted laterally in 1 bin increments and correlated with themselves at each step. For the

386  hairpin maze, in an analysis taken from Derdikman et al. (2009), we binned the place cell firing

387  rate map using a pixel size of 15 cm (the width of an arm) × 10 cm (along the arm in the vertical

388  dimension) and calculated the correlation between every possible pair of arms. These

389  correlation values were compared to correlations obtained when, for each cell, the firing rate

390  bins of each arm were shifted circularly by $\pm$ 150 cm or when the firing rate bins were reflected

391  along the x-axis. In all cases, correlations were only performed when the firing rate of both arms

392  was greater than 1 Hz. Finally, we modelled the activity of place cells in scale reproductions of

393  the square and circular spiral mazes used by Nitz et al. (2011). We then found the angle of each

394  place cell's fields relative to the centre of each environment, subtracted the circular median

395  value from these and removed the value closest to zero (or a random value if multiple values

396  were equally close to zero, which occurred if the circular median was the average of two

397  values). This process automatically excludes data from cells with less than 2 fields. We also

398  compared the angle of place fields between maze configurations.

399  **Results**

400  *Place fields repeat in four parallel alleyways*

401  As reported by Frank et al. (2000), Singer et al. (2010) and Grieves (2015), we observed

402  a high level of place field repetition in the four alleyway maze, which can be seen in the peaks of

403  the mean autocorrelation for all cells in this environment (Figure 6B). Arm correlation values

404  were significantly higher on average than shuffled ones ($z$ = 75.3, $p$ < .0001, $r$ = 0.87, WRSt, Md

405  = 0.99 and < 0.001 respectively) (Figure 6C). Example place cells can be seen in Figure 6D.
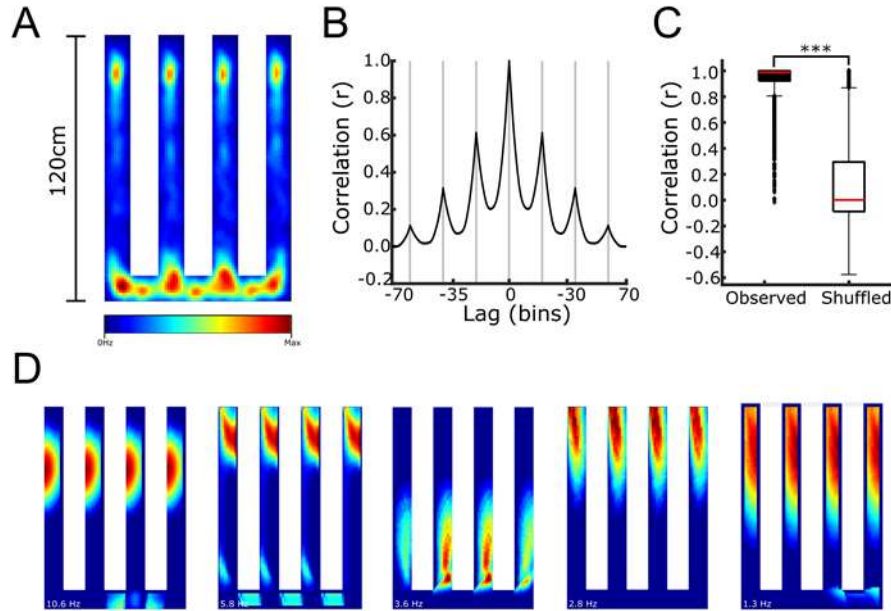
**Figure 6 A,** spatial map of all place fields detected in the four alleyway maze. **B,** mean and standard deviation linear autocorrelogram of all cells in the maze. Grey lines show the points at which alleyways overlap. **C,** median correlation either between arms of the maze (black box) or for a shuffled distribution where arms were compared to arm maps from other cells (open box). **D,** activity of five example place cells in this maze. Each exhibits repeating fields at similar locations along each alleyway. The number of BVC inputs these cells receive increases from left to right (2,3,4,6 and 7 inputs).

406        *Place fields repeat in a hairpin maze and turning points are overrepresented*

407        A different proportion of cells were active (firing > 1Hz) in our hairpin maze when

408    compared to an open field environment of the same size (1477 or 98.47% and 1202 or 80.13%

409    respectively; $x^2(1) = 28.23$, $p < .0001$, $\varphi_c = 0.02$, Chi-square test) and these cells also exhibited

410    a much higher number of fields in the hairpin maze ($z = 49.3$, $p < .0001$, $r = 0.82$, WRSt, Md =

411    10 and 1 respectively). The spatial distribution of place fields was also very different in these

412    two mazes. When comparing the top 37.5cm and bottom 37.5cm sections of the hairpin maze to

413    the middle 75cm zone, the majority of place fields in the hairpin maze were found in the top and

414    bottom sections (11084 (72%) and 4368 (28%) respectively; $x^2(1) = 2919$, $p < .0001$, $\varphi_c = 0.19$,

415    Chi-square test); this effect was not observed in the open field (845 fields (50%) and 853 fields

416    (50%) respectively, $x^2(1) = 0.04$, $p > .80$, $\varphi_c < 0.01$, Chi-square test) (Figure 7A, B and C).

417     Horizontal autocorrelations of the hairpin maze firing rate maps display clear peaks at a

418     shift of 0 (where the map overlaps with itself) but also at intervals of 30 bins (30 cm) where

419     alleyways with the same orientation overlap. Smaller peaks can also be seen at intervals of 15

420     bins (15 cm) where differently oriented alleyways overlap. Correlation values are higher at 30

421     bin than 15 bin intervals ($z = 51.1$, $p < .0001$, $r = 0.31$, WRSt, Md = 0.41 and 0.26 respectively)

422     and both are higher than corresponding values in autocorrelations performed on the open field

423     environment ($z = 113.7$, $p < .0001$, $r = 0.68$, Md = 0.41 and 0.0 respectively; $z = 82.3$, $p < .0001$,

424     $r = 0.31$, Md = 0.26 and 0.0 respectively, WRSt) (Figure 7D). The mean autocorrelogram for

425     each place cell shows a consistent effect throughout the vast majority of our place cells which

426     does not seem to be affected by the number of BVC inputs a place cell receives (Figure 7E).
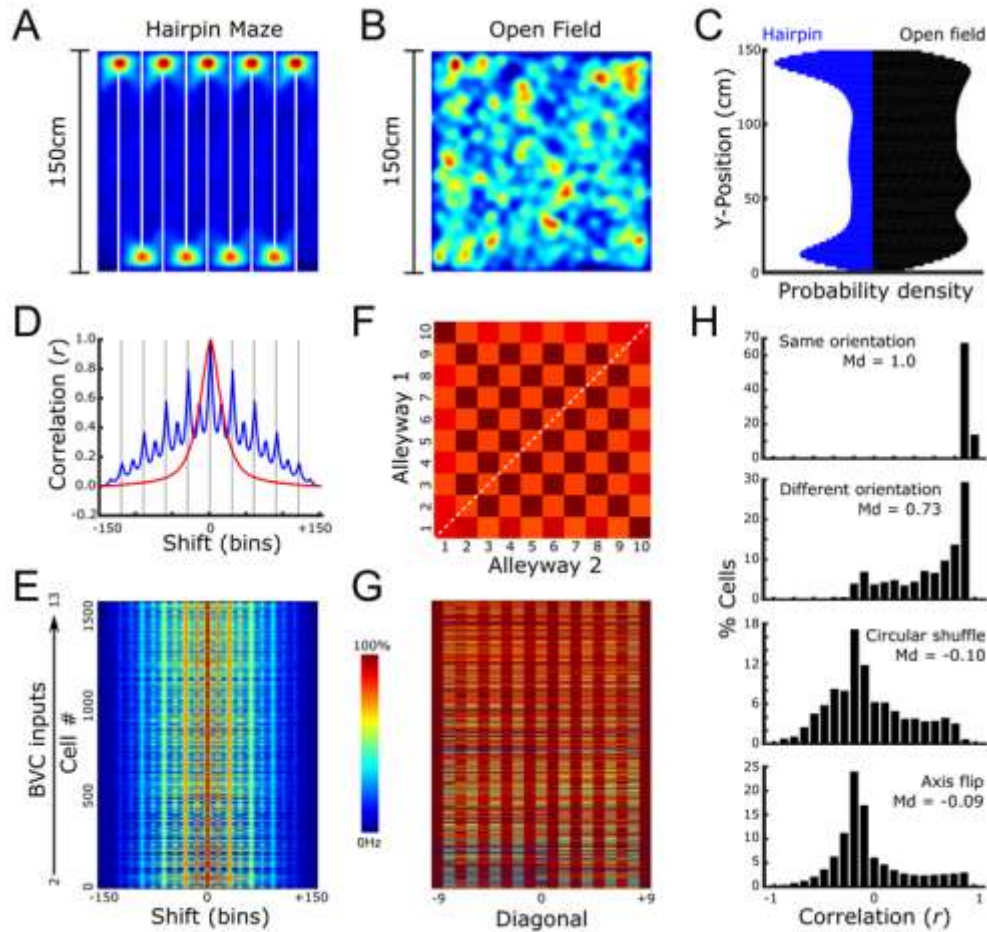
427

**Figure 7** Place cell activity in the Derdikman et al. (2009) apparatus. **A,** spatial map of all place fields detected in the hairpin maze. **B,** spatial map of all place fields detected in an open field with the same outer dimensions as the hairpin maze. **C,** violin plot showing the distribution of place fields along the y-axis in both the hairpin and open field apparatus. **D,** mean and standard deviation linear autocorrelogram of all cells in the hairpin maze (blue line) and in the open field (red line). Dotted lines show where the shifted hairpin maze alleyways line up with alleyways facing the same direction. **E,** linear autocorrelogram of all 1500 cells in the hairpin maze, one per row, these are arranged from cells with few to most BVC inputs. **F,** mean correlation matrix of all cells, each bin represents a comparison between two alleyways of the hairpin maze. The checkerboard pattern here resembles that reported by Derdikman et al. (2009) and indicates that those alleyways separated by an odd number of alleyways (i.e. alleyways facing the same direction) are more highly correlated. **G,** diagonal mean of each cell's correlation matrix, taken along the white dotted line shown in F, one cell per row, these are arranged as in E. **H,** distribution of correlation values obtained when comparing alleyways. The top graph shows the distribution when comparing odd or even alleyways (i.e. facing the same direction), the second graph shows the distribution when comparing odd to even alleyways (i.e. facing different directions), the third graph shows the distribution when comparing alleyways facing different directions after circularly rotating all odd numbered alleyways by a random number of bins and the bottom graph shows the distribution when comparing alleyways facing different directions after rotating all odd numbered alleyways 180° around their centre.

428        *Fields repeat only in alternating (odd or even) arms*

429        As reported by Derdikman et al. (2009), when we observed the results of arm

430   correlations as a matrix, a clear checkerboard pattern emerged, consistent with higher

431   correlation values for same orientation alleyways compared to different orientation ones (Figure

432   7F). In agreement with this, correlation values for same orientation alleyways were higher ($z =$

433   246.6, $p < .0001$, $r = 0.60$, WRSt, Md = 1.0 and 0.73 respectively). They were also higher than

434   shuffled distributions where each arm was randomly shuffled circularly ($z = 310.6$, $p < .0001$, $r =$

435   0.88, WRSt, Md = 1.0 and -0.10 respectively) or where alternating arms were reflected along

436   the x-axis ($z = 247.6$, $p < .0001$, $r = 0.87$, WRSt, Md = 1.0 and -0.09 respectively)(Figure 7H).

437   Again, the mean diagonal of each cell's correlation matrix shows that this effect was consistent

438   throughout most place cells, and the number of BVC inputs a place cell receives did not seem to

439   affect this (Figure 7G). Example BVCs and place cells can be seen in Figure 8.
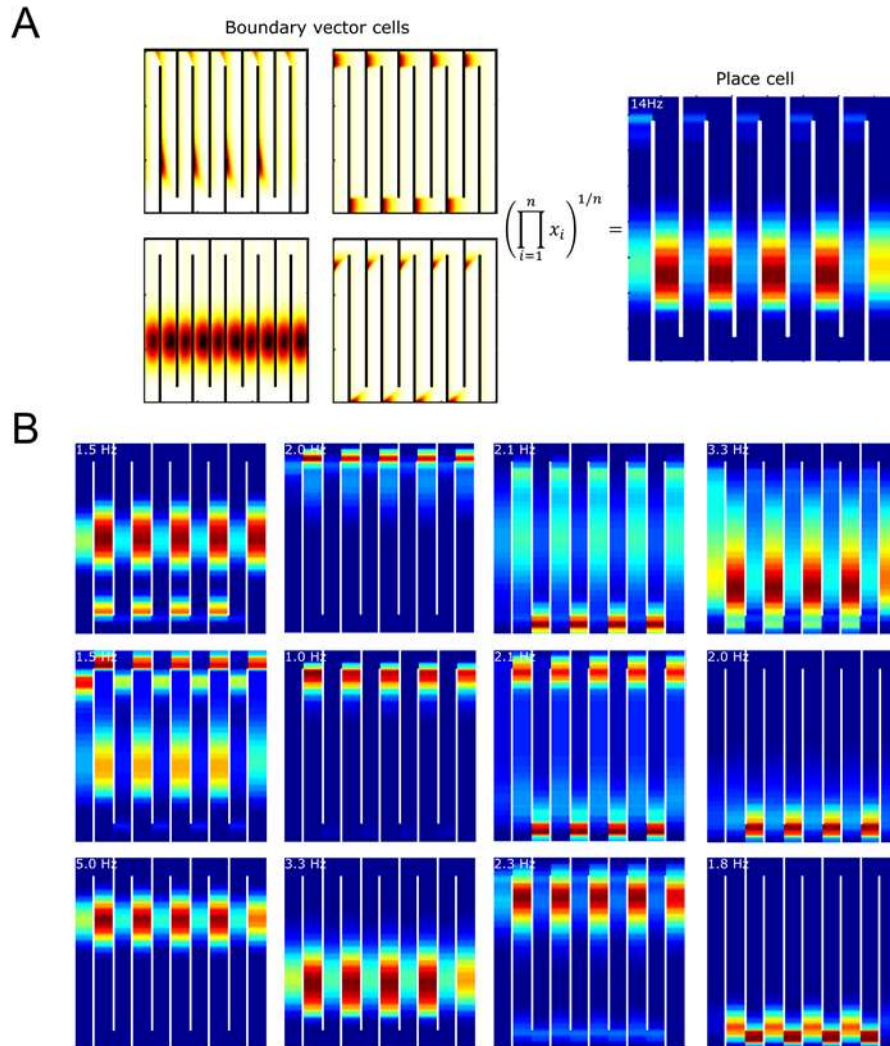
440

**Figure 8** Place cell activity in the Derdikman et al. (2009) apparatus. **A,** activity of four example BVCs in the hairpin maze (left) and activity of the place cell generated exclusively from these inputs (right). **B**, the activity of 12 more place cells in the hairpin maze, each exhibits repeating fields at similar locations along multiple alleyways that face the same direction. The number of BVC inputs these cells receive increases from top to bottom and from left to right (2 to 13 inputs; 13 inputs was the maximum utilised and only by one cell).

441         *Place cell characteristics are similar in a square and circular spiral, but fields in*

442         *the circular spiral get larger as loop size increases*

443         In the two spiral mazes we observed a different proportion of active (firing > 1Hz) cells,

444   but this was accompanied by a low effect size (1295 or 13.67% and 1418 or 5.47% respectively;

445   $x^2(1) = 5.48$, $p < .02$, $\varphi_c = 0.04$, Chi-square test). Cells also exhibited a different number of fields
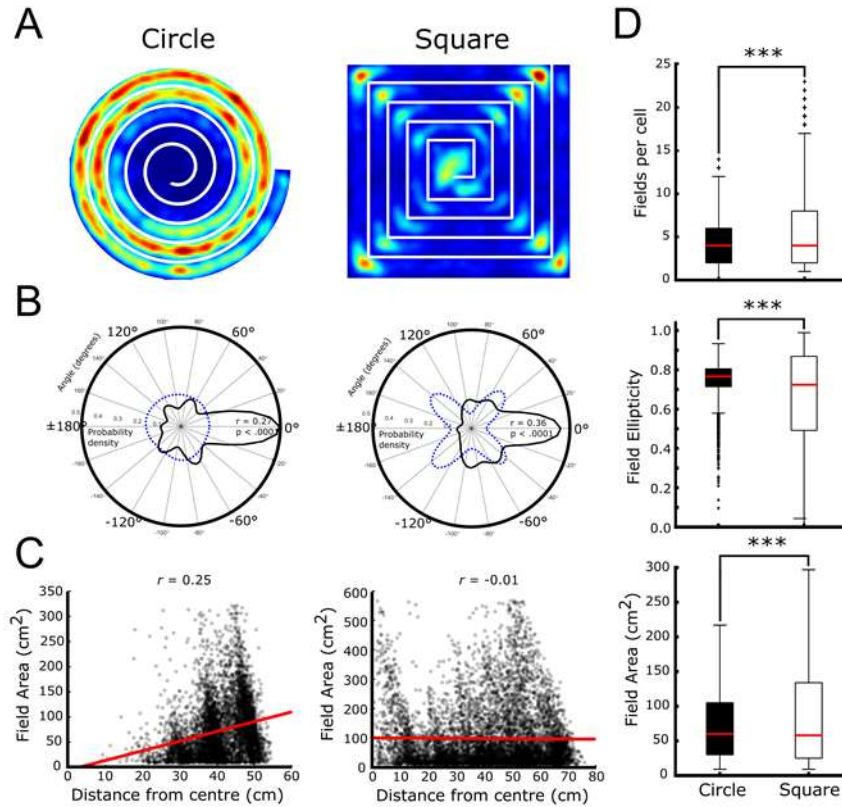
**Figure 9** Place cell activity in the Nitz (2011) apparatus. **A,** spatial map of all place fields detected in the spiral mazes. **B,** circular polar plots showing the position of all place fields in the circular spiral (left) and square spiral (right). This is expressed as the field's angle from the centre of the apparatus (blue dotted line) or when the median field angle for each cell is subtracted from all of its fields' values (black line). For the black line, an accumulation of fields around zero indicates that each place cell's fields lie on a radial line from the centre of the maze to the edge. **C,** density scatter graphs showing the size of all detected place fields in relation to their distance from the centre of the maze. **D,** boxplots showing place field statistics for the circular spiral (black boxes) and square spiral (open boxes). The top plot shows the median number of place fields per cell, the second plot shows the median ellipticity and the bottom plot shows the median place field area.

446  in each maze, but again with a low effect size ($z = 3.3$, $p < .0001$, $r = 0.06$, WRSt, Md = 4 in both

447  cases) (Figure 9D). Place fields were generally more elliptical in the circular maze than the

448  square one ($z = 10.5$, $p < .0001$, $r = 0.23$, WRSt, Md = 0.77 and 0.72 respectively) (Figure 9D).

449  Fields were also slightly larger in the circular maze ($z = -2.1$, $p < .05$, $r = -0.11$, WRSt, Md = 60

450  and 58cm$^2$ respectively) and fields increased in size linearly as the distance from the maze

451     centre increased ($r$(6479) = 0.25, $p$ < .0001), although not for fields in the square maze ($r$(7978)

452     = -0.01, $p$ > .30) (Figure 9C).

453

454            *Repeating fields are often found on a line from the centre of the spiral, turning*
455            *points in the square spiral are overrepresented*

456            In both the circular and square maze, fields were not unimodally distributed around the

457     centre ($r$ = 0.04 and $r$ = 0.06 respective Rayleigh vector tests). Moreover, when comparing the

458     frequency of fields at 90º offsets to those at 45º offsets we found that, in the square maze,

459     significantly more fields were distributed along 45º offsets than 90º ones ($t$(6) = 14.9, $p$ < .0001)

460     reflecting the geometry of the maze. The same relationship was not observed in the circular

461     maze fields ($t$(6) = -0.7, $p$ > .50, Figure 9B dashed blue lines). As reported by Nitz et al. (2011),

462     these results are in agreement with field clustering in the corners of the square maze alleyways

463     and can also be seen in a heatmap of all place fields on each maze (Figure 9A). However, when

464     we subtracted the median angle from each cell's field angles, the results clustered around zero

465     in both mazes ($r$ = 0.27 and $r$ = 0.36 respective Rayleigh vector tests; $v$ = 1337, $p$ < .0001 and $v$

466     = 2310, $p$ < .0001 respective non-uniformity V-tests, Figure 9B solid black lines). This confirms

467     that the majority of cells in these mazes have place fields which fall on a line from the centre of

468     the maze once their median angle is subtracted. Furthermore, when comparing the field angles

469     of cells in the two maze configurations the resulting correlation was significant ($r$(452) = 0.17, $p$

470     < .0005, Spearman's pairwise correlation) and the values were more similar than would be

471     expected by chance ($z$ = -5.0, $p$ < .0001, Wilcoxon signed rank test, Md = 39.68), indicating that

472     cells exhibited fields in similar locations on the two mazes. Example BVCs and place cells can
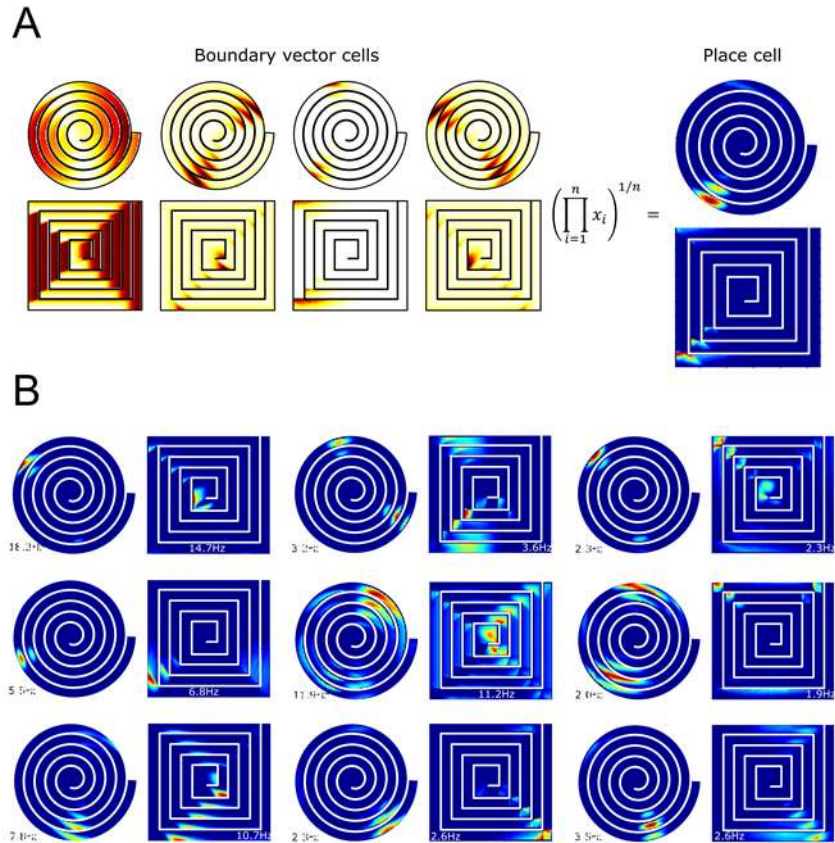
473     be seen in Figure 10.

474

**Figure 10** Place cell activity in the Nitz (2011) apparatus. *A,* the activity of four example BVCs in the spiral mazes (left) and the activity of the place cell generated exclusively from these inputs (right). *B,* the activity of 9 more place cells in the spiral mazes, each exhibits repeating fields that fall on a line drawn from the centre of the maze to the edge. The number of BVC inputs these cells receive increases from top to bottom and from left to right (2 to 10 inputs; 13 inputs was the maximum utilised and only by one cell).

### Discussion

475

476      We modelled the activity of place cells in a maze composed of four parallel alleyways,

477 and predicted that BVCs and modelled place cells would respond identically in each. This was

478 the case, confirming that activity does not require experience or learning to develop, and that it

479 can be explained by a geometric model of place cell firing.

480      As reported by Derdikman et al. (2009), in a multi-alleyway hairpin maze, modelled place

481 cells exhibited repeating fields only in alleyways with the same orientation. Furthermore, the

482 representations in alternating alleyways were not merely mirror images of each other,

483    confirming that a geometric model of place cell firing can account for this effect despite the very

484    small geometric change between alleyways. We also observed an overrepresentation of place

485    fields at the ends of the alleyways (i.e. at the turning points between alleyways). This seemed to

486    be due to the higher probability of BVC activity overlapping there and although not reported,

487    was one of the effects observed in the original study (D. Derdikman, personal communication).

488    One feature of the original data that the current model cannot support is the fact that place cells

489    in the original study exhibited completely different representations for left-right trajectories

490    through the maze compared to right-left trajectories. This effect can be thought of as analogous

491    to place field directionality in a linear track (McNaughton, Barnes, & O'Keefe, 1983) and is

492    unexplained by the current model, unless we consider that BVCs and place cells initialise a new

493    map for each running direction. A BVC model incorporating visual inputs (Raudies & Hasselmo,

494    2012), learning (Navratilova, Hoang, Schwindel, Tatsuno, & McNaughton, 2012) or contextual

495    information (Hayman & Jeffery, 2008) may better explain this effect.

496         Lastly, as reported by Nitz (2011) we found that, in a spiral maze, the majority of

497    modelled place cells exhibited repeating place fields, generally falling on a ray drawn from the

498    centre of the maze to the edge (i.e. appearing in multiple loops of the spirals where the rat

499    faced the same direction). Modelled place cells also exhibited firing features in common with the

500    observations of Nitz (2011). For instance, cells did not necessarily exhibit fields on all loops

501    (many cells did not have fields in the first or last loops) and fields in the square spiral track were

502    more elongated than those in the circular spiral. In the circular spiral maze, field area was also

503    strongly correlated with loop size (measured as distance from the maze centre) but in the

504    square maze this correlation was absent. Many cells in the square maze exhibited fields in the

505    corners of the square spiral that did not adapt their area to the size of the loop. This last result

506    simply seemed to be due to the higher probability of BVC inputs overlapping in the corners,

507    where two or more cells with near-perpendicular preferred firing directions can intersect. Lastly,

508 when comparing the square and circular spirals, place fields seemed to be present at the same

509 angle relative to the centre of the spiral in both mazes.

510 Nitz (2011) suggested that the BVC model could not explain the repeating fields

511 observed in these spiral mazes because cells should have fields in every loop. However, he

512 also pointed out that in the vast majority of these cases the missing field was located on the far

513 most outer or inner loops and we saw this same effect in our modelled data. This was probably

514 due different BVCs having different firing characteristics, meaning that while the activity of a set

515 of BVCs projecting to a place cell may overlap in several adjacent loops, this overlap diminishes

516 as the geometry of the loop diverges. Thus, the firing rates of adjacent place fields form a curve,

517 sloping downwards from the loop where BVC inputs combine most effectively. If this is centred

518 on a central loop then fields will be weaker or completely absent in more distant (i.e. inner and

519 outer) loops. Taken together, these results demonstrate that the BVC model does not need to

520 incorporate head direction or response sequences to explain place cell firing in spiral mazes.

521

## 522 Multicompartment mazes

523 Our primary hypothesis was that the place field repetition observed by Spiers et al.

524 (2015) in four parallel and visually identical compartments, as well as the absence of place field

525 repetition observed by Grieves et al. (2016b) in the same compartments when they were angled

526 away from each other, can be explained in terms of BVC inputs to hippocampal place cells. Our

527 prediction was that these same effects would be observable in a model of place cell firing based

528 solely on geometric inputs from BVCs. As earlier potential examples of place field repetition

529 were observed across mazes with two compartments, we also modelled two compartments

530 connected by a corridor (parallel; Skaggs and McNaughton (1998)) and two compartments

531 connected end to end (north to south; Tanila (1999). Together, these environments are

532 comparable to the environments used by Fuhs et al. (2005).

**Methods**

533

534        For the two compartment mazes, we used analyses described by Fuhs et al. (2005).

535 Firstly, we calculated the spatial correlation between the two compartments in the corridor

536 version of the task and between the two compartments in the opposite version (Figure 11A). For

537 the opposite configuration, we conducted analyses both with the bottom compartment rotated

538 180° or left unrotated. We also calculated compartment by compartment spatial correlations

539 between the two mazes, again both with the bottom compartment in the opposite configuration

540 rotated 180° or left unrotated. For each comparison, we also calculated an equivalent measure

541 between random cells without replacement. In all cases, a correlation was computed only if the

542 firing rate in each map was greater than 1 Hz. We also calculated the correlation between

543 maximum firing rates (peak value in the ratemap) in both compartments for each maze.

544        We note that the compartments in the opposite configuration of Fuhs et al. (2005) were

545 each rotated $\pm 90°$ relative to their counterpart compartments in the parallel configuration.

546 However, rats likely relied on local cues to orient themselves when placed in each maze

547 configuration, as both mazes were placed in the same curtained enclosure which did not contain

548 distal cues and the lighting was maintained evenly throughout environments. Fuhs et al. (2005)

549 reported that place cells from the majority of rats represented compartment 1 similarly in each

550 maze configuration if ratemaps for compartment 1 in the opposite configuration were first

551 rotated 90 degrees to match the parallel configuration. This suggests that when rats were first

552 introduced to the opposite configuration (always after experiencing the parallel configuration)

553 they oriented themselves using the first experienced compartment and visual cue. Thus, we

554 maintained the orientation of our modelled BVCs in each compartment 1, which is equivalent to

555 rotating Fuhs et al.'s (2005) parallel configuration maze +90 degrees.  This is reflected in the

556 orientation of maps in Figure 11A.

557        For the four compartment mazes we replicated the analyses used by Spiers et al. (2015)

558 and Grieves et al. (2016b). Firstly, we calculated the spatial correlation between each

559    compartment in the parallel maze to every other compartment. We did the same for the radial

560    maze but with all of the compartments rotated so that their longest axis was vertical, as in the

561    parallel maze, before correlating them. For comparison, we also conducted the same analysis

562    on pairs of maze compartments from random cells (where compartment identity was

563    maintained). We did this without replacement. We also performed a 1-dimensional lateral

564    autocorrelation on compartment firing rate maps concatenated edge to edge to form a single

565    map and we counted the number of place fields observed per cell in each environment. Lastly,

566    we calculated the spatial correlation between compartments in the two mazes (i.e. compartment

567    1 in the parallel maze vs compartment 1 in the radial maze) and for comparison we calculated

568    this correlation when the cells were shuffled but compartment identity was maintained. This was

569    also done without replacement. In all cases, a correlation was computed only if the firing rate in

570    each map was greater than 1 Hz. In both maze configurations, we observed a high number of

571    place fields in the doorways. To test if more fields were observed there than could be expected

572    by chance, we counted the number of fields found in the four doorway zones and compared this

573    number to those found in four equally sized zones distributed randomly throughout the

574    environment. We did this 1000 times, with control zones that were confined within the walls of

575    the maze and that could overlap.

576        One potential criticism of the analysis used by Grieves et al. (2016b) is that by rotating

577    the compartments in the radial configuration of the maze the relationship between boundaries

578    and place fields was disrupted, thus lowering any potential correlation in that maze. However,

579    Grieves et al. (2016b) detected place fields in their mazes and found an average of 1.12 (SEM =

580    0.06) place fields per cell in the radial configuration of their maze but 2.18 fields per cell (SEM =

581    0.18) in the parallel configuration (Grieves, 2015), suggesting that cells have more fields in the

582    parallel version rather than just repositioned fields in the radial maze. Nevertheless, to test this

583    hypothesis in our place cell population, we conducted the analyses described above on

584 'morphed' or reshaped radial maze compartments instead of rotating them, using the morphing

585 algorithm previously described in overall methods.

586 **Results**

587 *Place fields repeat in two parallel compartments but not in two opposite ones*

588 As reported by Fuhs et al. (2005), correlations between parallel compartments were

589 much higher than between opposite compartments. This was the case whether we rotated the

590 bottom compartment in the opposite configuration 180° ($D$(3000) = 0.96, $p$ < .0001, two-sample

591 Kolmogorov-Smirnov test, Md = 0.99 and -0.09 respectively) or not ($D$(3000) = 0.72, $p$ < .0001,

592 two-sample Kolmogorov-Smirnov test, Md = 0.99 and 0.60 respectively). However, without

593 rotation we did see a significant increase in correlation values ($D$(3000) = 0.58, $p$ < .0001, two-

594 sample Kolmogorov-Smirnov test, Md = -0.09 and 0.60 respectively) (Figure 11B). Firing rates

595 in the parallel configuration compartments were also more highly correlated than those in the

596 opposite configuration ($r$(1498) = 0.84, $p$ < .0001 and $r$(1498) = 0.55, $p$ < .0001 respective

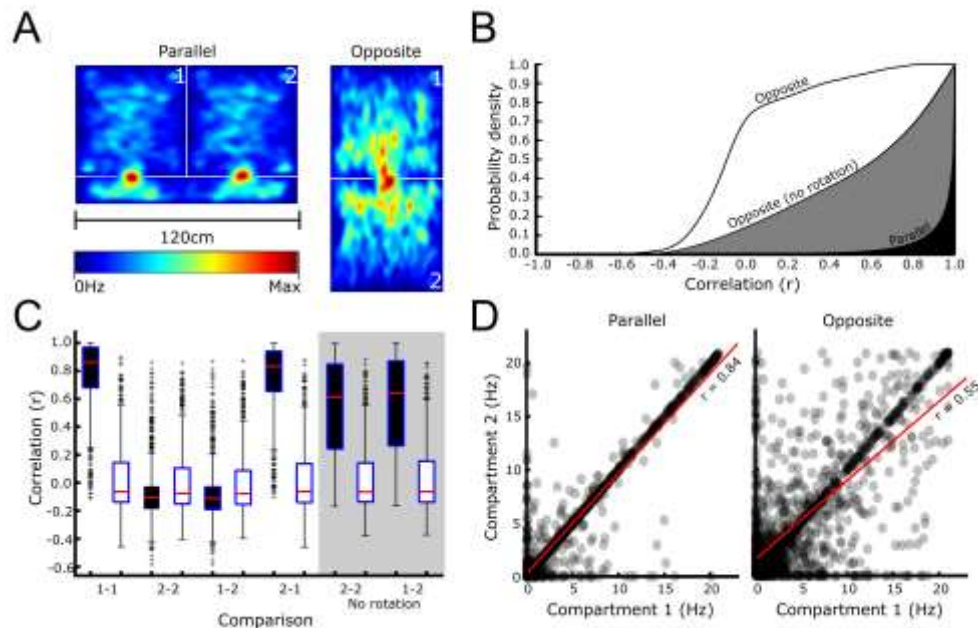597 Spearman's correlations) (Figure 11D).

598



32

**Figure 11** Place cell activity in the Fuhs et al. (2005) apparatus. *A,* spatial maps of all place fields detected in the two configurations of the maze. *B,* cumulative probability density functions for the correlation distributions found when comparing the compartments within each maze. Black shows the distribution when comparing compartments in the parallel configuration, white shows the distribution when comparing compartments in the opposite configuration after rotating compartment 2 by 180° to match compartment 1, grey shows the distribution when comparing compartments in the opposite configuration without rotating compartment 2. *C,* correlation distributions found when comparing compartments between the two maze configurations (i.e. compartment 2 in the parallel configuration to compartment 1 in the opposite configuration). The left eight boxes show the distributions after rotating compartment 2 in the opposite configuration by 180°, the four right boxes (on a grey background) show distributions without this rotation. *D,* density scatter plots showing the correlation (red line) between compartment firing rates (maximum in compartment ratemap) in the parallel (left plot) and opposite (right plot) maze configurations.

599          *Cells exhibit a distinct representation for the opposite compartment*

600          The four possible comparisons we made between the two mazes resulted in significantly

601     different correlation distributions whether compartment 2 in the opposite configuration was

602     rotated (H(3,3532) = 2461, *p* < .0001, Kruskal-Wallis test) or not (H(3,3532) = 410.4, *p* < .0001,

603     Kruskal-Wallis test). In either case, post-hoc tests confirmed that each distribution differed from

604     every other (*p* < .0001 in all cases) except comparisons between either parallel compartments 1

605     and 2 and opposite compartment 1 which were equally high (*p* > .05, Md = 0.86 and 0.83) and

606     comparisons between either parallel compartments 1 and 2 and opposite compartment 2 which

607     were equally low (with rotation: *p* > .05, Md = -0.10 and -0.11; without rotation: *p* > .05, Md =

608     0.61 and 0.64). Note that, when we rotated compartment 2 in the opposite configuration, the

609     correlation between this and compartments 1 and 2 in the parallel configuration decreased.

610     Indeed, this decrease was statistically significant for each (*p* < .0001 and *r* > 0.70 in both cases,

611     WRSt). These effects can be seen in Figure 11C. All distributions differed significantly from their

612     shuffled distributions (*p* < .05 in all cases WRSt) but with varying effect sizes (with rotation: *r* =

613     0.83, 0.83, -0.16, and -0.17; without rotation: *r* = 0.82, 0.64, 0.65 and 0.82). Shuffled

614     distributions did not differ whether compartment 2 was rotated (H(3,2989) = 6.91, *p* > .05,

615     Kruskal-Wallis test) or not (H(3,2975) = 0.89, *p* > .80, Kruskal-Wallis test) (Figure 11C).

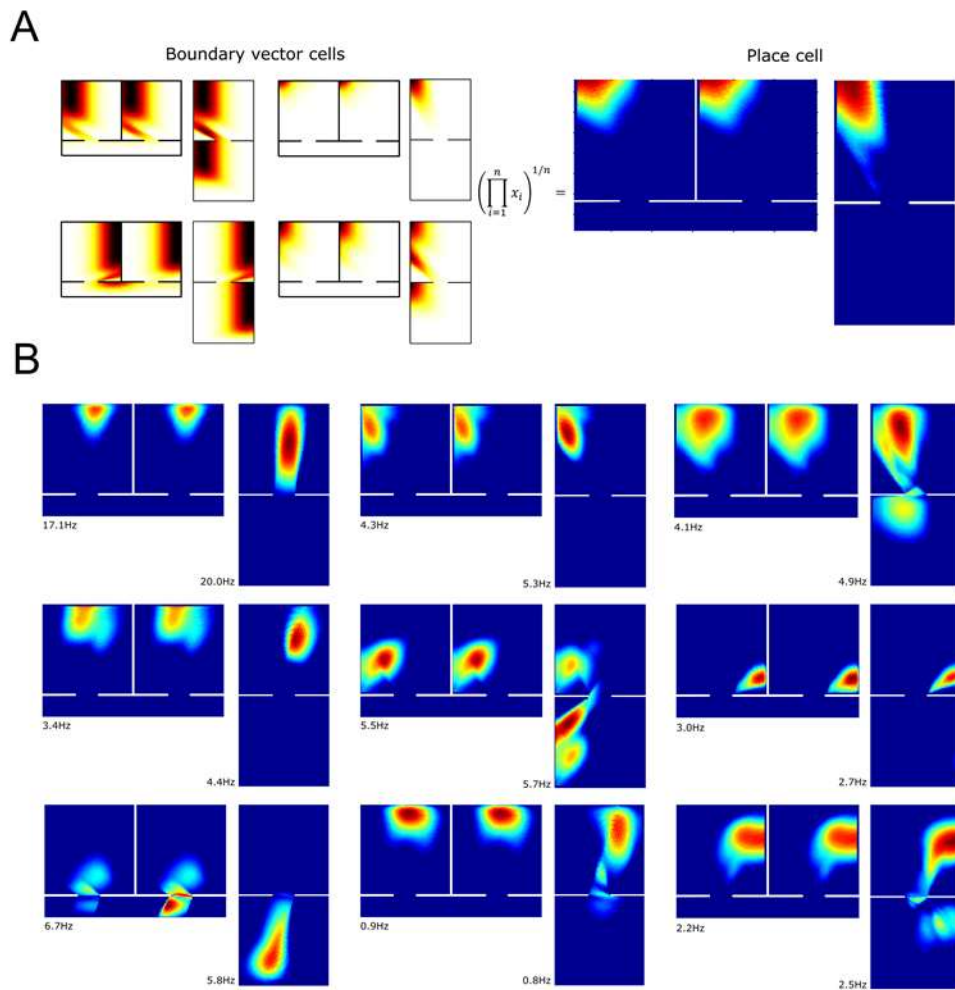616     Example BVCs and place cells can be seen in Figure 12.

**Figure 12** Place cell activity in the Fuhs et al. (2005) apparatus. **A,** activity of four example BVCs in the two compartment mazes (left) and activity of the place cell generated exclusively from these inputs (right). **B,** activity of 9 more place cells in the two compartment mazes, each exhibits repeating fields. The number of BVC inputs these cells receive increases from top to bottom and from left to right (2 to 10 inputs; 13 was the maximum utilised and only by one cell).

618       *Cells exhibit more fields in four parallel compartments than four radial ones, and*
619       *many of these are in doorways*

620       In the four compartment mazes we observed a similar proportion of active (firing > 1Hz)

621   cells in the parallel and radial configurations (1294 or 86.27% and 1302 or 86.80% respectively;

622   $x^2(1) = 0.03$, $p > .80$, $\varphi_c < 0.01$, Chi-square test). The number of place fields exhibited per cell in

623   each environment was significantly different, however, with a much higher number of fields

624  being exhibited by cells in the parallel configuration of the maze ($z = 18.26$, $p < .0001$, $r = 0.31$,

625  WRSt, Md = 4 and 2 respectively) (Figure 13E). In the parallel maze, 762 place fields (12.21%)

626  were observed in the four doorways. This number was significantly higher than the distribution

627  obtained from the random control points (99th percentile = 369, Md = 160, kernel smoothed

628  density estimated $p = 1.16 \times 10^{-41}$). The same effect was observed in the radial maze where 543

629  place fields (13.13%) were observed in the four doorways, significantly higher than in the

630  random control points (99th percentile = 302, Md = 79, kernel smoothed density estimated $p =$

631  $3.8 \times 10^{-25}$).

632

633      *Place cells repeat the same representation in four parallel compartments, but not*
634          *in four radial ones*

635          In the parallel maze, clear autocorrelation peaks can be seen at a shift of 0 but also at

636  intervals of 35 bins (35 cm) where different compartments overlap. Correlation values were

637  higher at 35 bin than 17.5 bin intervals ($z = 82.5$, $p < .0001$, $r = 0.67$, WRSt, Md = 0.49 and 0.01

638  respectively) and they were higher than corresponding values in autocorrelations performed on

639  the radial configuration ($z = 63.9$, $p < .0001$, $r = 0.39$, WRSt, Md = 0.01). In the radial data,

640  values at 35 bin intervals were also higher than those as 17.5 bin intervals but this was

641  accompanied by a lower effect size ($z = 16.5$, $p < .0001$, $r = 0.28$, WRSt, Md = 0.01 and 0.01

642  respectively) (Figure 13C). In the mean autocorrelogram for each place cell, this effect

643  appeared consistent throughout the vast majority of place cells and the number of BVC inputs a

644  place cell receives did not seem to affect this (Figure 13B).
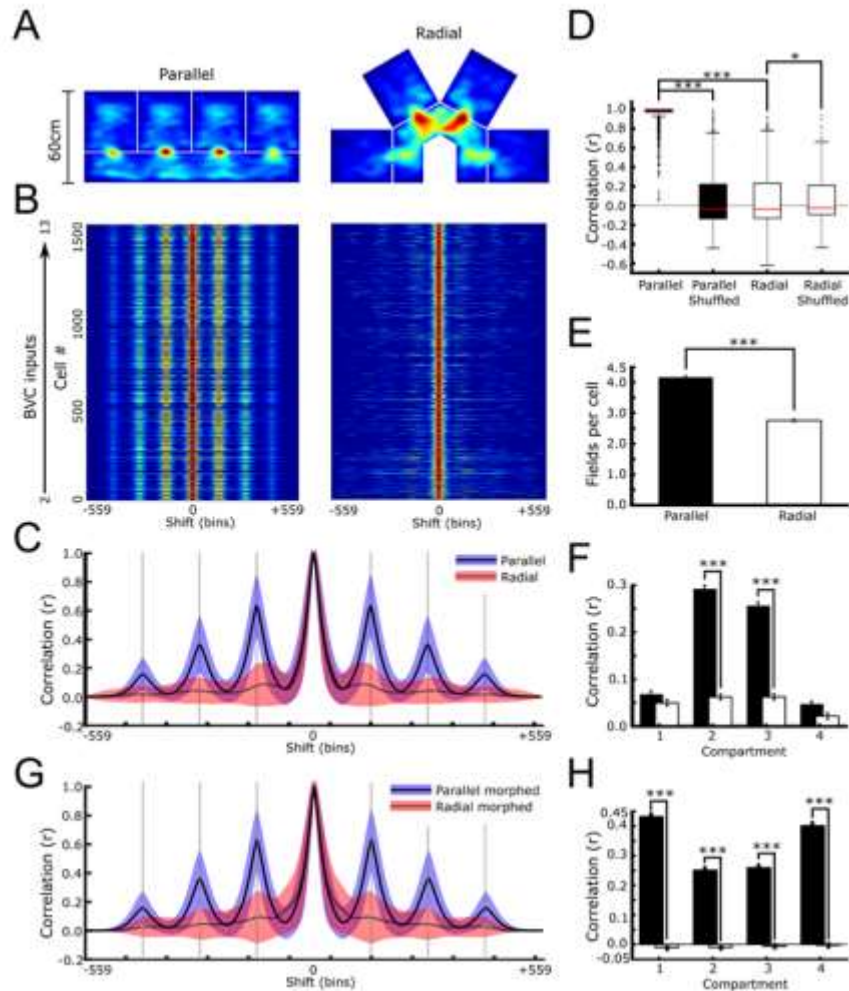
645

**Figure 13** Place cell activity in the four compartment mazes used by Grieves et al. (2016) and Spiers et al. (2015). *A,* spatial map of all place fields detected in the parallel (left) and radial (right) configuration of the maze. *B,* the linear autocorrelogram of all 1,500 cells in the parallel (left) and radial (right) configurations, one per row, arranged from cells with few to most BVC inputs. *C,* mean (black lines) and standard deviation (shaded areas) linear autocorrelogram of all cells in the parallel (solid line and blue area) and radial (dashed line and red area) mazes. A periodicity can be observed in the parallel autocorrelation but not in the radial, as reported by Grieves et al. (2016). *D,* within-maze compartment correlation distributions (black boxes) and the distributions obtained using shuffled compartment ratemaps (open boxes). The distributions are all centred on zero, with the exception of the distribution obtained from the parallel maze. *E,* average and SEM number of place fields per cell observed in each maze. *F,* between-maze compartment correlation distributions (black bars) and distributions obtained after shuffling these compartments (open bars). Only the correlations between compartments 2 and 3 are significantly above chance, these compartments are the most similarly oriented between the two mazes, with a 30º offset. *G,* same as C, but for morphed instead of rotated data. *H,* same as F but for morphed instead of rotated data. In this case, all compartments have significant correlations.

646    We next computed between-compartment correlations in the parallel and radial

647    configuration and a shuffled distribution for each. These differed significantly ($H$(3,7145) = 5060,

648    $p$ < .0001, Kruskal-Wallis test) and post-hoc tests confirmed that parallel maze values were

649    significantly higher than the other three distributions ($p$ < .0001 in all cases, Md = 0.99, -0.04, -

650    0.04 and -0.03 respectively). However, the shuffled parallel, radial and shuffled radial

651    distributions were all similarly low ($p$ > .90 in all cases)(Figure 13D). Inter-maze comparisons

652    (i.e. compartment 1 in parallel configuration vs compartment 1 in the radial configuration) were

653    not homogenous ($H$(3,1572) = 200.4, $p$ < .0001, Kruskal-Wallis test). Post-hoc tests confirmed

654    that each distribution differed from every other ($p$ < .0001 in all cases) with the exception of

655    comparisons between compartments 1 and 4, which were equally low ($p$ > .05, Md = -0.03 and -

656    0.04), and comparisons between compartments 2 and 3, which were equally high ($p$ > .05, Md =

657    0.30 and 0.21). When compared independently to shuffled distributions, only comparisons

658    between compartments 2 and 3 were significantly above chance ($z$ = 1.48, $p$ > .10, $r$ = 0.06, $z$ =

659    12.02, $p$ < .0001, $r$ = 0.41, $z$ = 10.47, $p$ < .0001, $r$ = 0.36 and $z$ = -0.28, $p$ > .70, $r$ = -0.03,

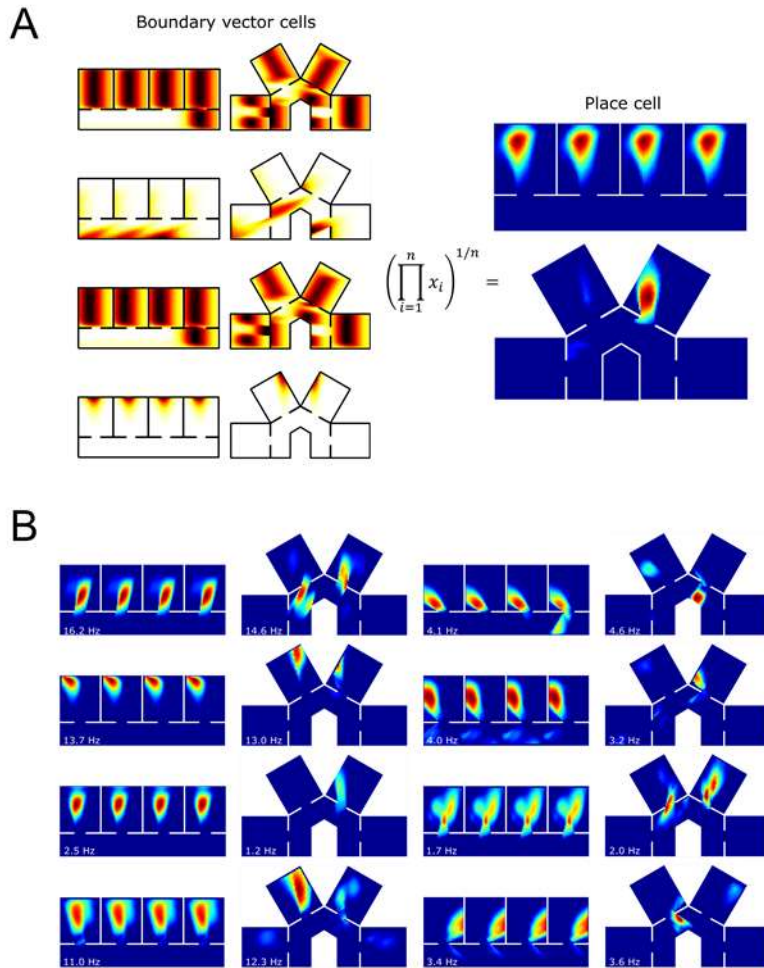660    respective WRSts, Figure 13F). Example BVCs and place cells can be seen in Figure 14.

661

**Figure 14** Place cell activity in the Grieves et al. (2016) and Spiers et al. (2015) apparatus. ***A,*** activity of four example BVCs in the two maze configurations (left) and activity of the place cell generated exclusively from these inputs (right). ***B,*** activity of 8 more place cells in these mazes, each exhibits repeating fields in the parallel configuration but not in the radial one. The number of BVC inputs these cells receive increases from top to bottom and from left to right (2 to 9 inputs; 13 was the maximum utilised and only by one cell).

662        *Rotating compartment maps decreases the correlation between them, but*

663        *morphed radial maze compartments are still less similar than parallel ones*

664        Correlations between mazes suggest that the compartments rotated by the least amount

665   (2 and 3 are rotated +30° and -30°, 1 and 4 are rotated +90° and -90° respectively) correlate

666   more highly. To test whether rotation itself results in lower correlations, we morphed

667   compartments in the radial configuration instead of simply rotating them. We also morphed the

668   parallel configuration maps but for this maze no statistical values differed from the rotated data

669   described above. Next, we performed a horizontal autocorrelation on concatenated

670   compartment ratemaps. In contrast to above, the morphed radial data values at 35 bin intervals

671   were not higher than those at 17.5 bin intervals ($z = 1.84$, $p > .06$, $r = 0.22$, WRSt, Md = 0.01

672   and 0.01 respectively)(Figure 13G). We then computed between-compartment correlations in

673   the parallel and radial configuration and a shuffled distribution for each. The resulting

674   distributions differed significantly ($H(3,7236) = 5130.7$, $p < .0001$, Kruskal-Wallis test) and post-

675   hoc tests confirmed that each distribution differed from each of the others ($p < .0001$ in all

676   cases), with the exception of the parallel shuffled and radial shuffled distributions ($p > .90$). The

677   morphed radial correlation distribution was higher than the one observed when the radial

678   compartments were rotated ($z = -23.56$, $p < .0001$, $r = -0.41$, WRSt, Md = -0.04 and 0.34

679   respectively) but it was still not as high as that obtained in the parallel maze ($z = 58.05$, $p <$

680   $.0001$, $r = 0.79$, WRSt, Md = 0.99 and 0.34 respectively). Inter-maze correlation distributions

681   differed significantly ($H(3,1599) = 76.3$, $p < .0001$, Kruskal-Wallis test) and post-hoc tests

682   confirmed that each distribution differed from every other ($p < .0001$ in all cases), with the

683   exception of comparisons between compartments 1 and 4 which were both high ($p > .99$, Md =

684   0.48 and 0.45) and comparisons between compartments 2 and 3, which were both

685   comparatively low ($p > .05$, Md = 0.19 and 0.20). When compared independently to shuffled

686   distributions, all comparisons were significantly above chance ($z > 12.0$, $p < .0001$ and $r > 0.40$

687   in all cases, WRSt). When compared to the distributions obtained when rotating, correlations

688   between compartments 1 and 4 were significantly higher when they were morphed rather than

689   rotated ($z = -16.85$, $p < .0001$, $r = -0.51$, WRSt, data for 1 and 4 combined, Md = -0.03 and 0.47

690   respectively), and the correlations between compartments 2 and 3 remain unchanged ($z = 1.48$,

691   $p > .10$, $r = 0.03$, WRSt, data for 2 and 3 combined, Md = 0.24 and 0.19 respectively) (Figure

692   13H).

**Discussion**

693

694        Many initial experiments studying place cell representations in similar environments

695    used two compartments connected by a doorway (Tanila, 1999) or alleyway (Skaggs &

696    McNaughton, 1998). Fuhs et al. (2005) used both configurations, so we sought to replicate their

697    experiment in our modelled data. As reported by Fuhs et al. (2005) and Skaggs and

698    McNaughton (1998), we found that in two parallel compartments connected by an alleyway,

699    modelled cells often fired similarly in both compartments. Also, as reported by Fuhs et al. (2005)

700    and Tanila (1999), we found that cells exhibited significantly more distinct representations for

701    each compartment in two compartments connected directly by an intervening doorway.

702        Like Fuhs et al. (2005), we found that compartment 1 in the opposite maze configuration

703    (top compartment in all diagrams) was represented highly similarly to both compartments in the

704    parallel configuration. The reason for this is clear when we consider the underlying BVC inputs:

705    since the orientation and geometry of this compartment is highly similar to the compartments in

706    the parallel configuration, both BVC and place cell representations are nearly identical.

707    However, in compartment 2, the shift of the doorway from the bottom to the top boundary largely

708    disrupts activity. In their within-maze analyses, Fuhs et al. (2005) rotated compartment 2 in the

709    opposite configuration by 180° before correlating this with compartment 1. They found that

710    correlations between these compartments were then much lower than those between

711    compartments in the parallel configuration. Again, our model provided the same pattern of

712    results. However, we also found that correlations calculated without the 180° rotation were

713    significantly higher (but still not as high as those in the parallel configuration), reflecting the

714    maintained preferred orientation of the underlying BVCs. Whether this relationship is also true in

715    the data of Fuhs et al. (2005) is unknown.

716        We modelled place cells in the four compartment apparatus used by Grieves et al.

717    (2016b) as this allowed us to replicate both Grieves et al. (2016b) and Spiers et al.'s (2015)

718    findings. Modelled place cells exhibited the same firing relationship and firing similarly in each of

719 four parallel compartments while exhibiting different representations in four radially arranged

720 ones. The underlying process is the same as before: because local orientation and geometry in

721 the parallel maze are highly similar for each compartment, BVC representations are nearly

722 identical in each. However, in the radial maze, the shift in the allocentric angles and positions of

723 the compartment walls and doorways disrupts this, resulting in divergent representations for

724 each compartment. In support of this, when comparing the compartments between mazes, we

725 found that correlations between compartments oriented similarly were significantly higher than

726 between compartments at very different orientations. This result was also reported by Grieves et

727 al. (2016b) and is easily explained using a geometric model: as the difference in orientation of

728 the compartments increases, the change in underlying BVC representations also increases

729 linearly.

730    However, this explanation suggests that the compartment rotation and correlation

731 methods employed here and by Grieves et al. (2016b) may be inappropriate. Perhaps place

732 cells represent compartments in the radial maze similarly, but as the compartments are rotated

733 for correlation the place field positions are similarly rotated out of place? This would artificially

734 reduce the similarity of compartments in the radial maze. Although it would not explain why

735 Grieves et al. (2016b) observed significantly more place fields in the parallel maze, a result we

736 have also replicated here. However, we sought to analyse our modelled data using an

737 alternative 'morphing' method. Instead of rotating compartments before calculating a spatial

738 correlation we morphed them into a new shape, thus preserving any allocentric spatial

739 relationships. We found that this method did in fact result in higher correlations in the radial

740 maze but these were still significantly lower than those in the parallel maze.

741    These results confirm that, to a certain degree, rotating compartments disrupts the

742 underlying geometric nature of place cell firing. However, correlations in the radial maze were

743 still lower than in the parallel maze. There are two possible reasons for this. First, as in the Fuhs

744 et al. (2005) maze described above, the position of the doorways in the radial maze also

745    disrupted the firing of cells in the different compartments. Each doorway was positioned at a

746    different angle to the centre of each box and morphing cannot rectify this disruption. This view

747    predicts that if the orientation or indeed the shape of the compartments in the parallel maze

748    were changed, the resulting correlations would be similar to those in the original parallel maze if

749    they were calculated using the morphing method (as long as the doorways would still be

750    positioned at the same angle relative to the centre of each box). Second, changing an

751    environment's geometry without changing its size will still lead to changes in BVC activity – even

752    if the environments are compared after morphing one to match the other. The reason for this is

753    that each place cell receives multiple BVC inputs. As these inputs are combined, small

754    geometric changes may lead to exaggerated changes in the place cell's activity. Thus, place

755    cells receiving a large number of BVC inputs are likely to have seemingly unpredictable

756    responses to environmental changes. Experiments seeking to show a predictable change in

757    place cell firing as evidence of a geometric model of place cell firing are at risk of failure unless

758    the precise nature of the underlying BVCs is estimated and used to model novel place cell firing

759    as in Barry and Burgess (2007).

760
761
## 762  Overall Discussion

763       *A minimalist, biologically tuned BVC model*

764       We used a modified version of the boundary vector cell (BVC) model of place cell firing

765    proposed by Hartley et al. (2000) and Barry et al. (2006) to test whether BVCs could account for

766    place cell behaviour in environments of different size or with repetitive elements. Our model

767    differs in a number of small, but meaningful ways. We combine BVC inputs using their

768    geometric mean rather than their linear sum, in an attempt to produce more realistic place cell

769    firing patterns. This approach seems to be necessary when modelling tighter, alleyway mazes,

770    which are rarely included in BVC models of place cell activity. This is likely due to the lower

771  probability of BVC firing fields overlapping in an alleyway environment for summation and

772  suggests that a multiplicative process may be more biologically plausible, despite its higher

773  complexity. An unexpected improvement is that very well spatially modulated place cells can be

774  generated using only two BVC inputs. We explored the effects of increased BVC inputs on place

775  field repetition and generated place cells with a variable number of BVC inputs. However,

776  provided that BVCs are chosen in a non-random process, whereby BVCs with similar preferred

777  firing distances and directions are less likely to project to a single place cell, we are confident

778  that realistic and well spatially modulated place cells can be reliably produced using very few

779  BVC inputs. Using only two BVCs allows many place cells to be generated from fewer BVCs

780  and requires fewer projections between the two cell populations.

781      In another alteration from the original models, we drew our BVC firing parameters from

782  continuous distributions which are biased towards more biologically realistic values. In previous

783  models, BVC preferred firing distances were drawn with equal probability from distances that

784  increased discretely in increasing steps. This method is indirectly biased towards returning

785  shorter distances. However, for greater control and transparency, we drew our BVC preferred

786  firing distances from a continuous, replicable distribution that is more strongly biased towards

787  returning short distances. The motivation for this is simply that the majority of boundary cells in

788  the subiculum and mEC are sensitive to environmental boundaries at short distances from the

789  animal. Nevertheless, we show that combining mainly short-distance BVCs in a multiplicative

790  way allows for realistic place fields that can themselves be distributed far away from

791  environmental boundaries. However, future modelling work would benefit greatly from closely

792  matching computational parameters to real, large scale biological datasets.

793

794      *The model predicts place field repetition in every case*

795      Using this model, we generated the firing of place cells in several open field,

796  multialleyway and multicompartment environments where place cells have been observed to

797    exhibit multiple, repeating representations. In each case, the repetition of place fields could be

798    explained almost entirely by BVC inputs to place cells, confirming that this phenomenon can be

799    driven by repeating, local geometric cues. These results further support the boundary vector cell

800    model of place cell firing. They also suggest that the firing of many place cells in the

801    hippocampus can be driven by simple, local cues and if this is the case these cells are unlikely

802    to form by themselves a global, cohesive 'cognitive map'.

803          Based on biological evidence there is good reason to believe this model is plausible; the

804    directional sensitivity of boundary cells rotate in unison with the preferred firing directions of

805    head direction (HD) cells and the grid orientation of grid cells (Perez-Escobar et al. 2016;

806    Solstad et al. 2008). When animals freely move between environments HD cells maintain the

807    same firing direction in each (Taube & Burton, 1995; Dudchenko & Zinyuk, 2005), thus we

808    would also expect boundary cells to maintain their firing relative to boundaries of a specific

809    orientation in connected environments. Indeed, in their two compartment experiment, Carpenter

810    et al. (2015) were able to record a medial entorhinal cortex boundary cell (see their

811    supplementary figure 1) which repeated the same boundary activity in the two parallel

812    compartments as predicted. This was further demonstrated in great detail by Brontons-Mas et

813    al. (2017), who inserted barriers into an open field to form four connected compartments

814    arranged in a square. Many subiculum boundary cells maintained a similar boundary sensitivity

815    in each compartment. Interestingly, not all of the boundary cells responded to the barrier inserts,

816    instead maintaining their firing relative to the original open field boundaries. In contrast, many

817    other cells were seemingly disrupted by the barriers. These interesting results demonstrate that

818    further research is needed into the characteristics and function of these underexplored cells.

819          This is apparent from recent research by Harland et al. (2017). They found that after

820    disrupting the activity of HD cells, place field repetition could be observed even in connected

821    compartments that place cells normally differentiate. It is unknown what effect disruption of the

822    HD system has on boundary cells. If they are unaffected we would need to know where they

823　gain their directional tuning from outside of the HD system. However, if boundary cells are

824　affected by HD system changes, it will be important to understand how place cells compensate

825　for this loss of input and it may suggest that BVC inputs are contextually gated, similarly to grid

826　cells.

827

828　　　　*Grid cells and contextual gating*

829　　　　We have not included grid cells in the current model. Instead, we see grid cells as a

830　means of contextual gating (Hayman, & Jeffery, 2008; Marozzi et al. 2015), allowing place cells

831　to overcome field repetition and form distinct representations for identical environments. This

832　view is supported by the finding that grid cells slowly develop a global representation for visually

833　identical, connected compartments (Carpenter et al., 2015) perhaps in line temporally with

834　learning in such environments and thus a decrease in place field repetition (Grieves et al.,

835　2016b). This contextual input could explain why Spiers et al. (2015) observed place field

836　remapping in one compartment of their maze upon changing its colour, despite continued

837　repetition in the others. Geometry and thus BVC inputs remained the same, but a contextual

838　change caused remapping in both grid and place cells only in that compartment. We would also

839　suggest that, as with other environmental cues, some place cells are likely driven more strongly

840　by geometric or contextual inputs, thus place field repetition may not be exhibited by all place

841　cells to the same extent. This also explains why spatial correlation values found in

842　multicompartment experiments form a distribution, centred on a high value but spread across a

843　range of values (Grieves et al., 2016b; Skaggs & McNaughton, 1998; Spiers et al., 2015).

844

845　　　　In summary, we present a purely geometric model of place cell firing which we have

846　used to replicate the activity of these cells in a number of published experiments. Together with

847　the behavioural and recording evidence indicating that the shape of the environment guides

848　spatial learning (e.g., Cheng, 1986; Gallistel, 1990; Hermer & Spelke, 1994; Learnmonth et al.,

849     2002; Hupbach & Nadel, 2005; Julian et al., 2015; Keinath et al., 2017; Weis et al., 2017), this

850     model suggests that geometry exerts a strong influence on spatial cognition. Our results show

851     that the field repetition activity of place cells observed in environments with similar or repetitive

852     geometric components, can largely be accounted for by boundary vector cell inputs.

853
854

855

856

# 857    Acknowledgements

862
863

# References

Alme, C. B., Miao, C., Jezek, K., Treves, A., Moser, E. I. & Moser, M-B. (2014) Place cells in the hippocampus: Eleven maps for eleven rooms. *PNAS*, 111(52), 18428–18435

Anderson, M. I., & Jeffery, K. J. (2003). Heterogeneous modulation of place cell firing by changes in context. *The Journal of Neuroscience: The Official Journal of the Society for Neuroscience*, *23*(26), 8827–8835.

Barry, C., & Burgess, N. (2007). Learning in a geometric model of place cell firing. *Hippocampus*, *17*(9), 786–800.

Barry, C., Lever, C., Hayman, R., Hartley, T., Burton, S., O'Keefe, J., Burgess, N. (2006). The boundary vector cell model of place cell firing and spatial memory. *Reviews in the Neurosciences*, *17*(1-2), 71–97.

Bjerknes, T. L., Moser, E. I., & Moser, M.-B. (2014). Representation of geometric borders in the developing rat. *Neuron*, *82*(1), 71–78.

Boccara, C. N., Sargolini, F., Thoresen, V. H., Solstad, T., Witter, M. P., Moser, E. I., & Moser, M.-B. (2010). Grid cells in pre- and parasubiculum. *Nature Neuroscience*, *13*(8), 987–994.

Bostock, E., Muller, R. U. & Kubie, J. L. (1991). Experience-dependent modifications of hippocampal place cell firing. *Hippocampus*. 1(2), 193-205

Brontons-Mas, J. R., Schaffelhofer, S., Guger, C., O'Mara, S. M. & Sanchez-Vives, M. V. (2017) Heterogeneous spatial representation by different subpopulations of neurons in the subiculum. *Neuroscience*. 343, 174-189

Burgess, N., Donnett, J. G., Jeffery, K. J., & O-keefe, J. (1997). Robotic and neuronal simulation of the hippocampus and rat navigation. *Philosophical Transactions of the Royal Society of London. Series B, Biological Sciences*, *352*(1360), 1535–1543.

Burgess, N., Jackson, A., Hartley, T., & O'Keefe, J. (2000). Predictions derived from modelling the hippocampal role in navigation. *Biological Cybernetics*, *83*(3), 301–312.

Bush, D., Barry, C., & Burgess, N. (2014). What do grid cells contribute to place cell firing? *Trends in Neurosciences*, *37*(3), 136–145.

Carpenter, F., Manson, D., Jeffery, K., Burgess, N., & Barry, C. (2015). Grid cells form a global representation of connected environments. *Current Biology: CB*, *25*(9), 1176–1182.

Cowen, S. L., & Nitz, D. A. (2014). Repeating firing fields of CA1 neurons shift forward in response to increasing angular velocity. *The Journal of Neuroscience: The Official Journal of the Society for Neuroscience*, *34*(1), 232–241.

Derdikman, D., Whitlock, J. R., Tsao, A., Fyhn, M., Hafting, T., Moser, M.-B., & Moser, E. I. (2009). Fragmentation of grid cell maps in a multicompartment environment. *Nature Neuroscience*, *12*(10), 1325–1332.

Dudchenko, P. A. & Zinyuk, L. E. (2005). The formation of cognitive maps of adjacent environments: Evidence from the head direction cell system. *Behavioral Neuroscience*. *119*(6), 1511-1523

Eichenbaum, H., Howard, E., Paul, D., Emma, W., Matthew, S., & Heikki, T. (1999). The Hippocampus, Memory, and Place Cells. *Neuron*, *23*(2), 209–226.

Frank, L. M., Brown, E. N., & Wilson, M. (2000). Trajectory encoding in the hippocampus and entorhinal cortex. *Neuron*, *27*(1), 169–178.

Fuhs, M. C., Vanrhoads, S. R., Casale, A. E., McNaughton, B., & Touretzky, D. S. (2005). Influence of path integration versus environmental orientation on place cell remapping between visually identical environments. *Journal of Neurophysiology*, *94*(4), 2603–2616.

Gallistel, C.R. (1990). *The Organisation of Learning*. Bradford Books/MIT Press.

Girardeau, G., Benchenane, K., Wiener, S. I., Buzsáki, G., Zugaro, M. B. (2009) Selective suppression of hippocampal ripples impairs spatial memory. *Nat Neurosci*, 12(10):1222-3.

Grieves, R. M. (2015, January 26). *The Neural Basis of a Cognitive Map*. University of Stirling. Retrieved from http://hdl.handle.net/1893/21878

Grieves, R. M., Wood, E. R. & Dudchenko, P. A. (2016a). Place cells on a maze encode routes

rather than destinations. *eLife*, 5:e15986. DOI: 10.7554/eLife.15986

Grieves, R. M., Jenkins, B. W., Harland, B. C., Wood, E. R., & Dudchenko, P. A. (2016b). Place

field repetition and spatial learning in a multicompartment environment. *Hippocampus*,

*26*(1), 118–134.

Grieves R. M., Duvelle É, Wood E. R. & Dudchenko, P. A. (2017b) Field repetition and local

mapping in the hippocampus and medial entorhinal cortex, *Journal of Neurophysiology*

(Forthcoming/Available Online)

Harland, B., Grieves, R. M., Bett, D., Stentiford, R., Wood, E. R. & Dudchenko, P. A. (2017)

Lesions of the Head Direction Cell System Increase Hippocampal Place Field Repetition,

*Current Biology*, 27(17), 2706-2712.

Hartley, T., Burgess, N., Lever, C., Cacucci, F., & O'Keefe, J. (2000a). Modeling place fields in

terms of the cortical inputs to the hippocampus. *Hippocampus*, *10*(4), 369–379.

Hayman, R. M., & Jeffery, K. J. (2008). How heterogeneous place cell responding arises from

homogeneous grids--a contextual gating hypothesis. *Hippocampus*, *18*(12), 1301–1313.

Hermer, L., & Spelke, E.S. (1994). A geometric process for spatial reorientation in young

children. *Nature, 370:* 57-59.

Hupbach, A., Nadel, L. (2005). Reorientation in a rhombic environment: no evidence for an

encapsulated geometric module. *Cognitive Development*, *20,* 279-302.

Jankowski, M. M., & O'Mara, S. M. (2015). Dynamics of place, boundary and object encoding in

rat anterior claustrum. *Frontiers in Behavioral Neuroscience*, *9*, 250.

Jankowski, M. M., Passecker, J., Islam, M. N., Vann, S., Erichsen, J. T., Aggleton, J. P., &

O'Mara, S. M. (2015). Evidence for spatially-responsive neurons in the rostral thalamus.

*Frontiers in Behavioral Neuroscience*, *9*, 256.

Julian, J.B., Keinath, A.T., Muzzio, I.A., & Epstein, R.A. (2015).  Place recognition and heading

retrieval are mediated by dissociable cognitive systems in mice*.  Proceedings of the

National Academy of Sciences*, *112(20)*, 6503-6508.

Keinath, A.T., Julian, J.B., Epstein, R.A., & Muzzio, I.A. (2017). Environmental geometry aligns

    the hippocampal map during spatial reorientation. *Current Biology*, *27,* 309-317

Kentros, C. G., Agnihotri, N. T., Streater, S., Hawkins, R. D. & Kandel, E. R. (2004) Increased

    Attention to Spatial Context Increases Both Place Field Stability and Spatial Memory.

    *Neuron*, 42(2), 283-295

Langston, R. F., Ainge, J. A., Couey, J. J., Canto, C. B., Bjerknes, T. L., Witter, M. P., … Moser,

    M.-B. (2010). Development of the spatial representation system in the rat. *Science*,

    *328*(5985), 1576–1580.

Learmonth, A.E., Nadel, L., & Newcombe, N.S. (2002). Children's use of landmarks:

    implications for modularity theory. *Psychological Science*, *13,* 337-341.

Leutgeb, S., Leutgeb, J. K., Barnes, C. A., Moser, E. I., McNaughton, B. L., & Moser, M.-B.

    (2005). Independent codes for spatial and episodic memory in hippocampal neuronal

    ensembles. *Science*, *309*(5734), 619–623.

Lever, C., Burgess, N., Cacucci, F., Hartley, T., & O'Keefe, J. (2002). What can the

    hippocampal representation of environmental geometry tell us about Hebbian learning?

    *Biological Cybernetics*, *87*(5-6), 356–372.

Lever, C., Burton, S., Jeewajee, A., O'Keefe, J., & Burgess, N. (2009). Boundary vector cells in

    the subiculum of the hippocampal formation. *The Journal of Neuroscience: The Official*

    *Journal of the Society for Neuroscience*, *29*(31), 9771–9777.

Lever C, Cacucci F, Burgess N, O'Keefe J. (1999). Squaring the circle: place cell firing patterns

    in environments which differ only geometrically are not unpredicatable. In *Society for*

    *Neuroscience Abstract* (p. 24:556).

Lever, C., Wills, T., Cacucci, F., Burgess, N., & O'Keefe, J. (2002). Long-term plasticity in

    hippocampal place-cell representation of environmental geometry. *Nature*, *416*(6876), 90–

    94.

Marozzi, E., Ginzberg, L. L., Alenda, A., & Jeffery, K. J. (2015). Purely Translational

Realignment in Grid Cell Firing Patterns Following Nonmetric Context Change. Cerebral

Cortex (New York, NY), 25(11), 4619–4627. http://doi.org/10.1093/cercor/bhv120

McNaughton, B. L., Barnes, C. A., & O'Keefe, J. (1983). The contributions of position, direction,

and velocity to single unit activity in the hippocampus of freely-moving rats. *Experimental*

*Brain Research. Experimentelle Hirnforschung. Experimentation Cerebrale*, *52*(1), 41–49.

Morris, R. G. M. (1981). Spatial localization does not require the presence of local cues.

*Learning and Motivation*, *12*(2), 239–260.

Muessig, L., Hauser, J., Cacucci, F. (2016) Place Cell Networks in Pre-weanling Rats Show

Associative Memory Properties from the Onset of Exploratory Behavior. *Cerebral Cortex*.

26(8), 3627–3636

Muessig, L., Hauser, J., Wills, J. T., Cacucci, F. (2015) A Developmental Switch in Place Cell

Accuracy Coincides with Grid Cell Maturation. *Neuron*. 86, 1167–1173

Muller, R. U., & Kubie, J. L. (1987). The effects of changes in the environment on the spatial

firing of hippocampal complex-spike cells. *The Journal of Neuroscience: The Official*

*Journal of the Society for Neuroscience*, *7*(7), 1951–1968.

Muller, R. U., Kubie, J. L., & Ranck, J. B., Jr. (1987). Spatial firing patterns of hippocampal

complex-spike cells in a fixed environment. *The Journal of Neuroscience: The Official*

*Journal of the Society for Neuroscience*, *7*(7), 1935–1950.

Navratilova, Z., Hoang, L. T., Schwindel, C. D., Tatsuno, M., & McNaughton, B. L. (2012).

Experience-dependent firing rate remapping generates directional selectivity in

hippocampal place cells. *Frontiers in Neural Circuits*, *6*, 6.

Nitz, D. A. (2011). Path shape impacts the extent of CA1 pattern recurrence both within and

across environments. *Journal of Neurophysiology*, *105*(4), 1815–1824.

O'Keefe, J. (1979). A review of the hippocampal place cells. *Progress in Neurobiology*, *13*(4),

419–439.

O'Keefe, J., & Burgess, N. (1996). Geometric determinants of the place fields of hippocampal

neurons. *Nature*, *381*(6581), 425–428.

O'Keefe, J., & Conway, D. H. (1978). Hippocampal place units in the freely moving rat: why they fire where they fire. *Experimental Brain Research. Experimentelle Hirnforschung. Experimentation Cerebrale*, *31*(4), 573–590.

O'Keefe, J. (1976). Place units in the hippocampus of the freely moving rat. *Experimental Neurology*, *51*(1), 78–109.

O'Keefe, J., & Nadel, L. (1978). *The hippocampus as a cognitive map*. Oxford University Press, USA.

Paz-Villagrán, V., Save, E., & Poucet, B. (2004). Independent coding of connected environments by place cells. *The European Journal of Neuroscience*, *20*(5), 1379–1390.

Peña, J. L., & Konishi, M. (2001). Auditory spatial receptive fields created by multiplication. *Science*, *292*(5515), 249–252.

Pérez-Escobar, J. A., Kornienko, O., Latuske, P., Kohler, L. & Allen, K. (2016) Visual landmarks sharpen grid cell metric and confer context specificity to neurons of the medial entorhinal cortex. *eLife*. eLife 2016;5:e16937

Peña, J. L., & Konishi, M. (2004). Robustness of multiplicative processes in auditory spatial tuning. *The Journal of Neuroscience: The Official Journal of the Society for Neuroscience*, *24*(40), 8907–8910.

Pfeiffer, E. & Foster, D. J. (2013) Hippocampal place-cell sequences depict future paths to remembered goals. *Nature*, 497, 74–79

Raudies, F., & Hasselmo, M. E. (2012). Modeling boundary vector cell firing given optic flow as a cue. *PLoS Computational Biology*, *8*(6), e1002553.

Savelli, F., Yoganarasimha, D., & Knierim, J. J. (2008). Influence of boundary removal on the spatial representations of the medial entorhinal cortex. *Hippocampus*, *18*(12), 1270–1282.

Schnupp, J. W., & King, A. J. (2001). Neural processing: the logic of multiplication in single neurons. *Current Biology: CB*, *11*(16), R640–2.

Sharp, P. E. (1997). Subicular cells generate similar spatial firing patterns in two geometrically

and visually distinctive environments: comparison with hippocampal place cells.

*Behavioural Brain Research*, *85*(1), 71–92.

Sharp, P. E. (1999). Subicular place cells expand or contract their spatial firing pattern to fit the

size of the environment in an open field but not in the presence of barriers: comparison with

hippocampal place cells. *Behavioral Neuroscience*, *113*(4), 643–662.

Singer, A. C., Karlsson, M. P., Nathe, A. R., Carr, M. F., & Frank, L. M. (2010). Experience-

dependent development of coordinated hippocampal spatial activity representing the

similarity of related locations. *The Journal of Neuroscience: The Official Journal of the*

*Society for Neuroscience*, *30*(35), 11586–11604.

Skaggs, W. E., & McNaughton, B. L. (1998). Spatial firing properties of hippocampal CA1

populations in an environment containing two visually identical regions. *The Journal of*

*Neuroscience: The Official Journal of the Society for Neuroscience*, *18*(20), 8455–8466.

Solstad, T., Boccara, C. N., Kropff, E., Moser, M.-B., & Moser, E. I. (2008). Representation of

Geometric Borders in the Entorhinal Cortex. *Science*, *322*(5909), 1865–1868.

Spiers, H. J., Hayman, R. M. A., Jovalekic, A., Marozzi, E., & Jeffery, K. J. (2015). Place field

repetition and purely local remapping in a multicompartment environment. *Cerebral Cortex* ,

*25*(1), 10–25.

Stewart, S., Jeewajee, A., Wills, T. J., Burgess, N., & Lever, C. (2014). Boundary coding in the

rat subiculum. *Philosophical Transactions of the Royal Society of London. Series B,*

*Biological Sciences*, *369*(1635), 20120514.

Tanila, H. (1999). Hippocampal place cells can develop distinct representations of two visually

identical environments. *Hippocampus*, *9*(3), 235–246.

Taube, J. S., Burton, H. L. (1995) Head direction cell activity monitored in a novel environment

and during a cue conflict situation. *Journal of Neurophysiology*, *74*(5), 1953-1971

Thompson, L. T., & Best, P. J. (1989). Place cells and silent cells in the hippocampus of freely-

behaving rats. *The Journal of Neuroscience: The Official Journal of the Society for Neuroscience, 9*(7), 2382–2390.

Weiss, S., Talhami, G., Gofman-Regev, X., Rapoport, S., Eilam, D., Derdikman, D. (2017). Consistency of spatial representations in rat entorhinal cortex predicts performance in a reorientation task. *Current Biology, 27*, 3658-3665.

Thompson, L. T., & Best, P. J. (1990). Long-term stability of the place-field activity of single units recorded from the dorsal hippocampus of freely behaving rats. *Brain Research*, *509*(2), 299–308.

Wills, T. J., Barry, C., & Cacucci, F. (2012). The abrupt development of adult-like grid cell firing in the medial entorhinal cortex. *Frontiers in Neural Circuits*, *6*. https://doi.org/10.3389/fncir.2012.00021

Wilson, M. A., & McNaughton, B. L. (1993). Dynamics of the hippocampal ensemble code for space. *Science*, *261*(5124), 1055–1058.

Yoganarasimha, D., & Knierim, J. J. (2005). Coupling between place cells and head direction cells during relative translations and rotations of distal landmarks. *Experimental Brain Research. Experimentelle Hirnforschung. Experimentation Cerebrale*, *160*(3), 344–359.